Educational simulation of the electroencephalogram

Grit, M.B.M.

Award date:
1997

Educational Simulation of the Electroencephalogram

M.B.M. Grit

Thesis on the masters project performed by M.B.M. Grit, id.nr 356124
for the MBS group, Eindhoven University of Technology,
under supervision of P.J.M. Cluitmans, Ph.D.

The work was performed from December 15 1996 until august 15 1997
at the Florida Anesthesia Computer Engineering Team (FACET), Department of Anesthesiology, School of Medicine, University of Florida, Gainesville, USA,
under supervision of N.A.M. de Beer, Ph.D., and W.L. van Meurs, Ph.D.

Summary

Anesthesia protects patients undergoing surgical procedures from unnecessary pain and damage by inducing unconsciousness and analgesia, and by monitoring vital organs. The electroencephalogram (EEG) is monitored for the interpretation and management of the stages of anesthesia and for the early revelation of hypoxia or damage to the brain. The Human Patient Simulator (HPS) is a full-scale patient simulator that consists of a patient-like mannequin that exhibits clinical signs and responds to therapeutic interventions in a realistic way. A neurophysiological extension of the HPS will be used for teaching anesthesia residents the handling of EEG monitoring equipment, the effects of anesthesia on the EEG, the effects of surgery on the EEG, and the differentiation of these effects.

As a basis for the simulation of EEGs, an existing signal generator is described. This model-driven EEG signal generator simulates EEG signal components rather than the neuronal structure underlying the signal. The signal generator allows independent variation of the power or amplitude in each of the conventional EEG frequency bands. This is obtained by filtering a Gaussian white noise in five different bands, each with its independent variable gain. As a part of the Masters project, the frequency transfers of the five band filters are designed to resemble representative peaks in the frequency spectrum of real human EEGs. Peaks in these real EEGs are parametrized and these parameters are used as the requirements for the filter frequency characteristics. The parameters are fitted by means of a narrow ideal bandpass filter, combined with a Hann window. According to anesthesiologists with EEG monitoring experience, the patterns simulated with the EEG signal generator in which these filters are implemented, look like typical EEGs and bear enough resemblance to actual EEGs to be used for educational simulation. As a foundation for the modeling of drug effects on the EEG, the current insights in pharmacokinetic and pharmacodynamic modeling are summarized. A compartment model is used to predict the apparent effector site concentration, the effector site in this case being the brain. Drug effects on the EEG are modeled as a function of this concentration. From information about the effects of the important intravenous hypnotic propofol on the EEG, resulting from a literature search, a piece-wise linear relation between the propofol effector site concentration and the EEG effects is derived. A simulation of the effects of propofol with this model showed that it was necessary to shift the delta band filter towards lower frequencies. According to three anesthesiologists with EEG monitoring experience, a simulation of the effects of propofol with the modified delta filter is realistic enough for educational simulation. A second modeled drug effects is burst suppression: an alternating pattern of EEG bursts and silences. In order to facilitate the extraction of burst suppression parameters from the scientific literature, the existing burst suppression model is modified. Suppression ratio and suppression duration are modeled as a linear function of the effector site concentration. In the chosen model the (dependent) burst duration is also a linear function of the concentration. According to an EEG expert burst suppression is simulated realistically enough for educational simulation.

For the implementation of scenarios like carotid endarterectomy, the EEG simulator has to be extended with a second channel, the effects of damage and different stages of hypoxia in the brain, and the effects of body temperature on the EEG. The addition of more drugs to the model will enlarge its field of application. The ultimate educational value of the EEG simulator has to be formally evaluated, with the help of clinical instructors in a controlled training environment. Possible future application areas for an EEG simulator, based on the current design, are the

simulation of epileptic seizures, EEG monitoring of patients with head trauma in the ICU, and EEGs during various sleep stages.

SUMMARY

1. INTRODUCTION 1

2. ANESTHESIA AND THE ELECTROENCEPHALOGRAM 2

2.1 Anesthesia 2

2.2 The Electroencephalogram 3
origin of the EEG 3
measuring the EEG 3
EEG classification/describing the EEG 4
artifacts in the raw EEG 5

2.3 Anesthesia and the EEG 6

3. TEACHING EEG MONITORING BY SIMULATION 8

3.1 Anesthesia Education and Simulation 8
elements of anesthesia education 8
anesthesia simulation 8

3.2 Full-Scale Patient Simulators 9
the UF METI Human Patient Simulator 9
full-scale patient simulator design considerations 10

3.3 Learning Objectives for a Neurophysiological Module 11

4. EEG MODEL AND FILTER DESIGN 14

4.1 Existing Model Structure 14
EEG simulator 15
EEG model 15
signal generator 16
display 16

4.2 Filter Design for the Signal Generation Model 17
signal generation model 17
signal and frequency spectra requirements 19
anticipated future requirements 19
implementation requirements 19
filter selection and implementation 20
filter parameter estimation 22
simulation results 23

5. MODELING OF DRUG EFFECTS ON THE EEG 25

5.1 Pharmacokinetic models 25
pharmacokinetics 25
exponential model 26
compartment model 27

clinical model 28
apparent effector site concentration 28

5.2 Modeling Drug Effects on the EEG **29**
pharmacodynamics 29
modeling the spectral amplitudes 29
modeling burst suppression 32

6. CRITICAL MODEL EVALUATION: INTEGRATION OF PROPOFOL **33**

6.1 The Effects of Propofol on the EEG **33**
pharmacokinetics of propofol 33
modeling the band gains 34
modeling burst suppression 36

6.2 Initial Simulation Results and Model Modifications **37**
pharmacokinetics 37
gains 37
modification to the basic model 41
burst suppression 41

6.3 Expert Evaluation of the Updated Model **43**
gains 43
burst suppression 47

7. CONCLUSIONS AND RECOMMENDATIONS **49**

8. REFERENCES **51**

1. Introduction

This report describes the masters project performed as part of the study of Electrical Engineering at the Eindhoven University of Technology. The mission of the Medical Electrical Engineering section of the department of Electrical Engineering is to develop and apply technological principles from Electrical Engineering and Information Technology to contribute to the improvement of the quality and cost-effectiveness of health care. Among the focuses of the section are techniques for anesthesia and neurophysiology. The focus on these fields has led to a long-standing collaboration with the Florida Anesthesia and Computer Engineering Team (FACET), in which the masters project was performed. FACET is part of the Department of Anesthesiology at the University of Florida in Gainesville, USA. It conducts interdisciplinary research in biomedical and health care technology, facilitates clinical and basic research, and actively engages in medical education. The FACET objective is to integrate computer applications, engineering technology, and medicine to improve the state-of-the-art of health care in general, and anesthesia in particular.

One of FACET's achievements is the (ongoing) development of the Human Patient Simulator (HPS). The HPS is a full-scale patient mannequin that is used as an educational tool allowing physicians, residents in training, medical students, and allied health-care personnel to practice evaluation and treatment of pathological situations without risk to real patients. The present version of the HPS exhibits clinical signs (such as palpable pulses and heart sounds), a computer controlled mechanical lung that inhales and exhales real gases, and mathematical (software) models of patient physiology and pharmacology that make the simulated patient respond in a realistic fashion to treatment. The vital signs of the simulated patient are displayed on standard monitoring equipment. In order to allow training of situations that include brain function monitoring, a neurophysiological module is currently being added. This enhancement of the HPS will result in the simulation of EEG signals, integrated with current simulation scenarios.

The masters project consisted of the development of parts of the neurophysiological module and is described in this thesis. To get acquainted with the essentials of anesthesia, the EEG, and the use of EEG monitoring during anesthesia, an introduction to these topics is given in chapter 2. Part of the project was to describe the derivation of learning objectives for the neurophysiological module from educational considerations and simulator design considerations. This description is given in Chapter 3. Also part of the project was the formal description of the basic EEG simulation model design. One of the elements of this model, the actual EEG signal generator, includes five band filters. The formal design of these filters was part of the masters project. Chapter 4 describes the basic model and the filter design. The current insights in pharmacokinetic and pharmacodynamic modeling are summarized in chapter 5, taking an engineering perspective. The existing drug effect model of the EEG simulator, also described in chpater 5, is based on this knowledge. A literature search on the effects of propofol on the EEG was performed. The implementation of propofol in the EEG simulator is used as a critical evaluation of this model, to reveal whether it is also applicable to other drugs, and whether it is feasible to obtain the model parameters from the literature. Chapter 6 describes the results of the literature search and the implementation of propofol into the model. It also describes the modifications that had to be made to the existing model and a new burst suppression model. Conclusions and recommendations can be found in chapter 7.

2. Anesthesia and the Electroencephalogram

During surgical procedures anesthesia is used to protect patients from unnecessary pain and damage. Since too large doses of anesthetic drugs, on the other hand, can be harmful, anesthesiologists need to be able to monitor the state of anesthesia and the working of the vital organs during anesthesia. One of the monitoring tools is the electroencephalogram, which represents brain activity. In this chapter an introduction on anesthesia and the electroencephalogram will be given and the use of the electroencephalogram during anesthesia will be elucidated.

2.1 Anesthesia

Most of the information, given in this section is based on [VanderAa-90].

In order to be able to perform medical procedures with as little damage to the patient as possible, anesthesia is applied. More precisely, anesthetic drugs are administered in order to induce a state of analgesia (insensitivity to pain), unconsciousness, amnesia (loss of memory), and non-responsiveness to noxious stimulation. Many drugs influence a number of these aspects simultaneously. The recent development of specific drugs for the different aspects of anesthesia makes it possible to manipulate the different aspects independently. Besides the use of muscle relaxants, which were already known for their specific working, analgesia and amnesia can also be manipulated independently. Propofol can for example be used as a hypnotic, inducing mainly unconsciousness and amnesia, and alfentanil as a specific drug to induce mainly analgesia.

A state of general anesthesia is obtained by administration of drugs intravenously or through inhalation. Anesthesia consists of three steps: induction, maintenance and emergence. Prior to surgery the anesthesiologist visits the patient in order to decide what anesthetic procedure to use. This decision is based on an evaluation of the patient's history and current condition, current use of drugs and specific medical problems.

Induction of anesthesia is achieved by administration of rapid acting and short lasting intravenous drugs or through inhalation of a mixture of oxygen and an anesthetic with the help of a face mask. In order to prevent movement during operation, the patient's muscles are relaxed with the help of muscle relaxants, making it difficult or impossible for the patient to breathe independently. Therefore the patient will have to be mechanically ventilated. Ventilation is started after a process called tracheal intubation during which a tube is placed in the trachea of the patient. Tracheal intubation is made easier by administration of a brief acting muscle relaxant during induction, just after the patient has lost consciousness.

When the patient is safely connected to the ventilator, the medical procedure may be performed by the surgeon. The anesthesiologist's task is to maintain anesthesia at a level with the least risk to the patient, while allowing for the medical procedure to take place. This can be obtained by administering drugs intravenously or with the help of the anesthesia machine which controls the composition of the gas mixture that is administered to the patient. During the maintenance period, the anesthesiologist monitors the working of the vital organs and the overall safety of the patient. If necessary he will change the administration doses of anesthetics in order to maintain a constant level of anesthesia.

The anesthesiologist has a number of features at his disposal to monitor anesthetic effects. Classic features are characteristics of respiration, pupil size, the eyelid reflex, other clinical signs such as

swallowing and vomiting, and tear production. Besides the pupil size and tear production these features have lost their value since the introduction of muscle relaxants. Other features such as the systolic blood pressure, heart rate, sweating, the electromyogram, the EEG, and evoked potentials are useful indicators of the effects of anesthesia.

After the medical procedure has come to an end, the anesthesiologist ends the administration of anesthetics and initiates a reversal of the induced anesthetic state with drugs that counteract the effects of the administered anesthetics. This stage of anesthesia is called emergence. The patient will then be transported to the recovery room where the remaining drugs will have the chance to be assimilated by the body. The patient is monitored during his recovery until full awakening to assure that no complications will emerge.

Another form of anesthesia is regional anesthesia, which includes spinal, epidural, nerve and field blocks. Regional anesthesia does not produce loss of consciousness or amnesia.

2.2 The Electroencephalogram

Administration of the right amounts of anesthetic drugs is an art, rather than a science. The anesthesiologist has no exact feed-back about the state of analgesia, amnesia and hypnosis and the variability of the effects of drugs on different patients is very large. In addition, the level of anesthesia can be altered by surgical events, such as incision. The anesthesiologist has, however, some indicators of the state of anesthesia at his disposal. The electroencephalogram (EEG) is one of them.

origin of the EEG

The electroencephalogram represents the electrical effect of brain activity at different positions at the scalp. Neuronal activity in the brain is accompagnied with changing potentials. Since the amplitude of these potentials decreases rapidly with increasing distance from the neurons that produce them, the EEG only represents the activity of the neurons in the outer layer of the brain, called the cortex.

If the neurons in the brain would fire randomly, the summation of the electrical activity at the scalp would cancel out, since the number of neurons is very large. Groups of brain cells in the cortex, however, receive input from the same underlying structures, causing coherence in their activity. This coherent activity will result in measurable electrical activity at the scalp.

An EEG typically shows rhythmic activity. This rhythmic behavior is supposed to be caused by the way the neurons in the cortex are activated by the thalamus. The connections between thalamus and cortex impose a certain frequency on their firing. The changes in this frequency are directly reflected in the frequency of the (dominant) rhythmicity of the resulting EEG.

measuring the EEG

The EEG is recorded by placing electrodes on the scalp. For electrode placement, conventions such as the international 10-20 system, according to which the electrodes are placed at distances of 10 or 20 % of the cranium, are used (see figure 2.1). Electrodes are indicated with a combination of a letter (sometimes two) and a number. The letter indicates the part of the cortex under the electrodes position. P stands for parietal, F for frontal etc.. Electrodes over the left hemisphere (left side of the brain) have odd numbers, electrodes over the right hemisphere have even numbers. The midline electrodes are indicated with a "z". The electrodes A1 and A2 at the ear lobes are usually used as reference, either as single reference, or in combination using A1 +A2 as reference. Fpz is usually used as the signal ground.

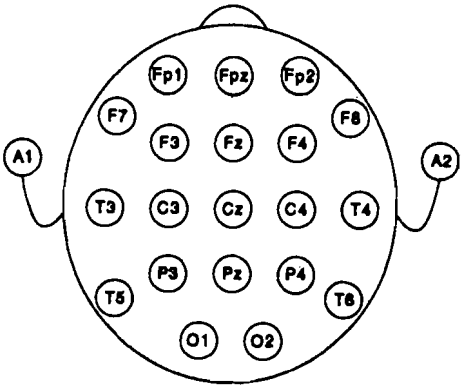

Figure 2.1: illustration of 10-20 system (from [DeBeer-96], permission granted by author)

The placing of the electrodes, the processing (filtering and amplifying) of the signal and the grounding during EEG measurement can substantially influence the resulting EEG signal.

EEG classification/describing the EEG

In order to describe and classify the measured EEG, a number of techniques and methods have been developed. Classification can be based on the raw EEG as presented on a screen or on EEG features resulting from EEG processing. Derivation of EEG features can be performed on-line or the EEG signal can be stored for off-line processing for research purposes.

From the raw EEG in the time-domain the number of zero-crossings per second (zero-crossing frequency, ZXF) can be counted. The zero-crossing frequency is used as an indicator of the mean frequency of the EEG signal during a considered time interval.

Many other methods of describing the EEG are based on the frequency spectrum of the signal. In order to describe an EEG signal, the frequency spectrum is usually divided into four distinct bands, ranging from delta to beta corresponding to 0 to 30 Hertz, as indicated in table 2.1 (sometimes subdivisions of these bands such as the division of beta into beta-1 and beta-2 are used). Anesthesiologists and other EEG-experts classify the frequencies that are present in the EEG into these bands and describe them with their amplitude. A normal awake, relaxed person with eyes closed, for example, will have an EEG with a prominent alpha rhythm and a lower-amplitude beta combined with small amounts of theta. Opening the eyes will block or attenuate the alpha rhythm so that the dominant frequency will be in the beta range with a small amount of theta activity. See figure 2.2 for an example of an awake baseline EEG signal.

Table 2.1 frequency bands used in EEG classification

band	frequency range (Hz)
delta	0-4
theta	4-8
alpha	8-13
beta-1	13-20
beta-2	20-30

Figure 2.2: awake baseline EEG

In addition to a classification of the EEG by means of the amplitude of the dominant frequencies in bands, signal processing techniques make it possible to use the distribution of the power across the various bands. The absolute and relative power of each band can be calculated. The ratio of the power of typical bands can be calculated as well. A much used power ratio is the delta ratio which is calculated by dividing the power in the delta band by the power in the beta band.

Other features derived from the raw EEG are the characteristic frequencies. The spectral edge frequency (SEF) is defined as the frequency in the EEG spectrum above which no significant amount of power (3-5% of the total power) is present. The median (power) frequency (MF or MPF) is defined as the frequency above or below which 50% of the total power is present. The peak power frequency (PPF) is the frequency at which the largest amount of power is present in the spectrum.

A fairly new method is bispectral analysis [Sigl-94]. Besides the power of the various frequencies present in the signal, it is also determined whether quadratic non-linearities exist in the EEG. When two components of frequencies X and Y are present in the EEG, then presence of quadratic nonlinearities will result in the power of frequencies X-Y and X+Y being dependent on the power of the component frequencies X and Y. Bispectral analysis is combined with other features of the EEG in the BIS, the bispectral index. Several studies have shown that the bispectral index correlates strongly with the traditional EEG characteristic frequencies and that it might have a strong relation to depth of anesthesia (e.g. [Kearse-94]).

artifacts in the raw EEG

The raw EEG can be influenced or disturbed by various artifacts. These artifacts influence the EEG and can therefore influence the various EEG-features. Usually the raw EEG is checked manually for artifacts and only those parts of the EEG that are artifact-free are used for analysis. Artifacts can be caused by various sources as enumerated by [DeBeer-96].

Electromyographic (EMG) activity. Contraction of a muscle results in electrical activity that can be recorded with surface electrodes. Especially contraction of neck and jaw muscles will interfere with EEG recording at scalp electrodes. Because the frequency content of the EMG lies in the 100-300 Hz range, filtering of the EEG will usually be sufficient to remove this type of artifact. A side-effect of muscle relaxants during anesthesia is the effective elimination of EMG artifacts.

Eye movement. Because the eye can be considered an electrical dipole, eye movements will change the electrical activity that is recorded at scalp electrodes.

Electrocardiogram (ECG). The electrical activity of the heart can often be picked up by EEG electrodes on the scalp. Interference from a cardiac pacemaker may result in very large ECG artifacts. Usually ECG artifacts are minimized by choosing a symmetrical point for the reference electrode, for example on the subject's forehead.

Electrode movement. The cause of this type of artifact was already discussed in the previous section, where possible ways of preventing electrode movement artifacts were mentioned, namely thoroughly fixing the electrodes in place on the skin, and choosing an electrode material in which the electrochemical equilibrium between electrolyte and skin will quickly restore itself.

Mains interference. The most common cause of mains interference (50-Hz in Europe, 60 Hz in the United States), is unequal electrode impedances. This was already discussed in the section about measuring the EEG. When attempts at equalizing electrode impedances are not sufficient to eliminate all mains interference, a notch filter at 50-60 Hz may be used, but only if this does not remove part of the signal of interest.

Electrosurgery. Electrosurgical equipment sometimes generates very strong, high-frequency electrical fields that can be picked up by EEG and ECG electrode leads. This type of interference is often so strong that the EEG amplifiers overload, resulting in an output signal that is absolutely useless. Obviously, in the case of amplifier overload this type of interference is impossible to filter out, and the only way to deal with this type of artifact is to stop EEG monitoring during periods in which electrosurgery is used.

2.3 Anesthesia and the EEG

The amplitude and frequency of cortical potentials vary with changing levels of cerebral function, and are particularly influenced by the state of the metabolism. More specifically they vary with the use of (anesthetic) drugs and disease-related alterations of cerebral functions. These changes that are dependent on the overall level of consciousness are made visible by the EEG. Although the reason for rhythmicity and simultaneous firing of neurons is not clear at this moment, experience with alterations in the EEG makes possible an interpretation and management of the depth of sedation and the stage of anesthesia by continuous EEG-recording. During operations, events such as hypoxia or ischemia in (a part of) the brain or dysfunctioning of the brain in general can be revealed early, so intervention can take place in order to prevent or minimize actual damage.

For a number of reasons it is not possible to give a standard relation between the stage of anesthesia and the EEG. First of all, there is a variety in the reaction to drugs between patients, the so-called inter-patient variability. Second, the stage of anesthesia is dependent on external factors, such as arousal by surgical procedures. Third, each drug has its particular influence on the EEG. Some patterns in the EEG seem to have almost general validity for various drugs. During induction of anesthesia usually delta activity increases. Beta activity increases initially but will decrease with higher concentrations.

Overall the EEG shows "slowing" which is also illustrated by the fact that the MPF decreases with increasing drug concentrations [Schwilden-89].

For high concentrations of anesthetic drugs burst suppression may occur. Burst suppression consists of diffuse high-amplitude bursts alternating with periods of low amplitude EEG or even EEG silence (iso-electricity). See figure 2.3 for an illustration of a burst suppression pattern.

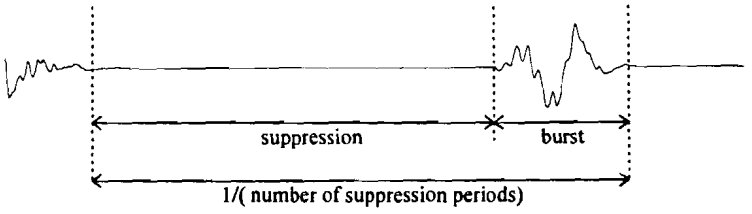

Figure 2.3: Burst suppression EEG

Thiopental, for example, shows an increase in beta activity after administration. With increasing blood concentrations in the brain this beta activity decreases again and alpha activity takes it place. Theta and delta activity increase as well. With even higher concentrations, activity in all bands decreases, resulting in dominant delta activity. For high concentrations of thiopental, burst suppression occurs [Bührer-94].

Scientists are still searching for a general drug-independent measure of the depth of anesthesia (consciousness or amnesia) using the EEG. Some attempts do have some success, but up until now, no satisfying measure is found.

An inverse relation between the zero-crossing frequency of the spontaneous EEG and anesthetic concentrations has been established, but proved not to be a useful measure of awakening during recovery. The spectral edge frequency follows changes in anesthetic concentrations. The SEF and median power frequency (MPF) seem to be good measures for the transition from anesthesia to recovery, but their large variability makes them less useful. The bispectral index is found to correlate strongly with the traditional EEG characteristic frequencies. In studies where it was attempted to predict movement in response to incision, the bispectral index performed slightly better in predicting movement, but slightly worse in predicting absence of movement, when compared to spectral edge frequency, median frequency, or other EEG spectral features.

The EEG is also influenced by body temperature and oxygen level in the brain. For low temperatures, the EEG shows slowing, becoming iso-electric for very low temperatures. A lack of oxygen shows a similar effect.

3. Teaching EEG Monitoring by Simulation

As part of the master's project a formal description of the deduction of the learning objectives and design considerations for a neurophysiological module was made, resulting in this chapter.

Anesthesiologists and other medical personnel have to be trained before they can work with real patients. Education takes the form of theoretical courses, practical exercises on patients under supervision of experts, and -more recently- by working with training devices and simulators. This chapter will discuss some elements of what anesthesiologists need to learn. An elaboration will be given on one new educational modality: a (full-scale) simulator. One specific full-scale simulator, the UF METI Human Patient Simulator (HPS), will be treated in more detail, followed by some full-scale simulator design considerations. Finally, the learning objectives for a neurophysiological module for this HPS are formulated.

3.1 Anesthesia Education and Simulation

Education of anesthesiologists consists of a number of elements and can be achieved by a number of modalities. This section gives a brief description of elements of anesthesia education and focuses on one teaching modality: simulation.

elements of anesthesia education

Anesthesiologists have to learn how to achieve and maintain certain levels of sedation, amnesia, analgesia, and muscle relaxation. At the same time they have to learn how to maintain a patient's state so that the organs function normally and are not damaged.

In order to obtain these skills anesthesiologists in training have to learn the differential diagnosis and management of clinical problems. They have to learn to make a distinction between different clinical signs such as drug effects, equipment malfunction, organ dysfunction, and artifacts and their impact on monitored signals and variables. Preferably these skills are taught without risk to real patients.

Education should start with training specific learning objectives. Most suited for this type of training are specific training devices. After the basic skills are taught, they can be combined in a more complex training with a full-scale anesthesia or patient simulator.

anesthesia simulation

A simulator is defined as a device that enables the operator to reproduce or represent under test conditions phenomena likely to occur in actual performance [Webster's-90].

Simulators allow education of anesthesiologists without any risk to real patients. A simulator offers the possibility to perform certain procedures many times, improving the skills in equipment handling and the insight in the effects of the procedures before they are applied to real patients. In addition, simulation offers the possibility to train uncommon situations. During their education anesthesiologists might never encounter these situations and when occurring in the OR, they are normally taken out of their hands, preventing the trainee from ever dealing with such situations during their education. Another advantage of simulators is the possibility to make leaps in time. Intubation and extubation can be trained, e.g., without dealing with the (long) intermediate period of

maintenance during surgery. Simulators are also well suited for training of crisis management and team training [Gaba-95].

One of the dangers of the use of simulators lies in the fact that the users of simulators mix up reality with simulation. [Lees-96] gives the example of a pilot that almost taxied from the taxiway. The pilot had recently experienced training in a flight simulator under nearly identical circumstances using taxiway center lighting which exists in the simulator for that taxiway at that airport, but not in reality.

3.2 Full-Scale Patient Simulators

An advanced form of anesthesia simulation is full-scale patient simulation. Full-scale patient simulators consist of a patient-like mannequin that realistically shows clinical signs and responds to (clinical) actions in a realistic way. As an example of a full-scale patient simulator the UF METI Human Patient Simulator is treated, followed by some general full-scale patient design considerations.

the UF METI Human Patient Simulator

The Department of Anesthesiology at the University of Florida has developed (and continues to develop) a full-scale human patient simulator (see figure 3.1). This simulator is commercially available as the University of Florida Medical Education Technologies Inc. Human Patient Simulator, UF METI HPS. Below a description of the main elements of the HPS is given, based on [Good-93]. This description is not exhaustive, it is merely a description of the elementary parts.

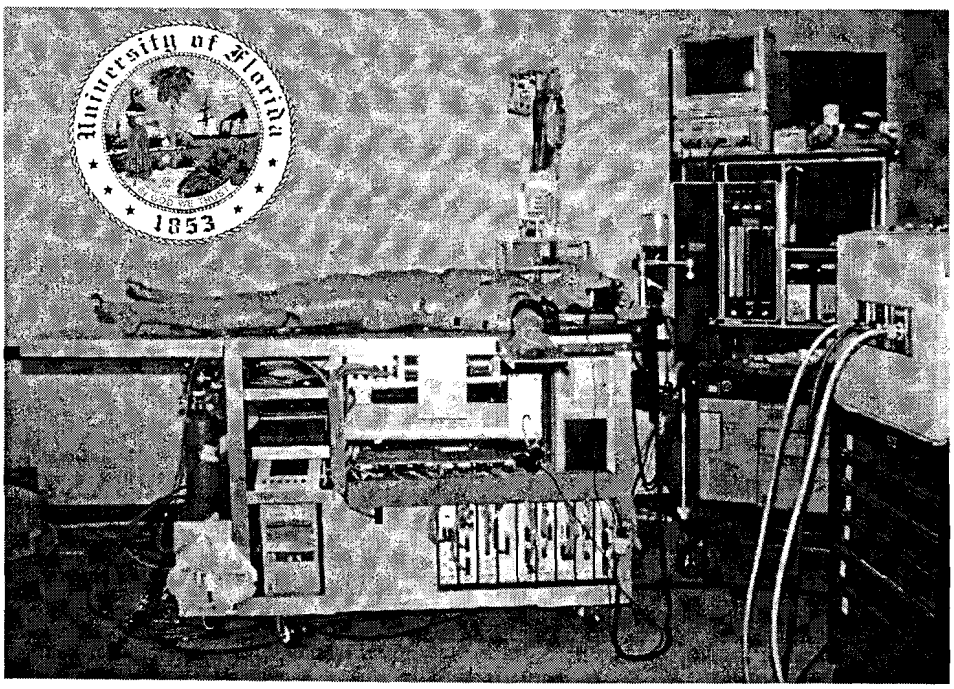

Figure 3.1: The Human Patient Simulator

The patient is represented physically by a mannequin. The model of the head and neck include an anatomically shaped pharynx and larynx, enabling laryngoscopy and different kinds of ventilation. Several parts of the airway can be manipulated, offering the possibility to simulate a wide range of real airway problems. It is possible to perform transtracheal ventilation on the simulator if the airway is blocked.

Clinical signs and monitored signals of the cardiovascular system are represented in a number of ways. The simulator's carotid and radial pulsations are palpable, and heart sounds can be heard with a stethoscope at the chest. The ECG is measured at chest electrodes and shown on a monitor. In addition a number of blood pressures is shown on monitors. The blood pressures, the sound and the palpable pulsations are all synchronized with the ECG.

The lungs of the HPS consist of a computer controlled mechanical lung that inhales and exhales real gases. The composition of the gases in the mechanical lung (alveolar gases) is analyzed and transmitted to a computer model. This model calculates the rate of oxygen consumption, the rate of carbon dioxide production, and the uptake or elimination of anesthetic gases. The result of these calculations are transmitted to the physical portion of the lung model, which uses a gas substitution technique to physically add or remove gases from the alveolar gas space. Spontaneous inhalation or artificial ventilation with or without anesthetic gases will automatically affect the alveolar gases and the different models will react appropriately resulting in a realistic exhaled gas mixture. The mechanical lung model allows variation of a number of parameters, such as airway resistance. The lungs breathe spontaneously, until the muscles are relaxed, after which the lungs can be ventilated mechanically. The chest of the HPS moves up and down with each respiratory cycle. Lung sounds can be heard over the lungs through speakers in the chest.

A thumb of the HPS reacts to nerve stimulation by a peripheral nerve stimulator. The twitch height is a function of the administered amount of muscle relaxant.

A pharmacologic computer model determines the effects of drugs at different sites in the body. Volatile agents are detected in the lungs as described above. The bar-code on the syringes with intravenous drugs tells the model what the administered drug and its concentration are, and the amount of administered drugs is measured.

The anesthesia equipment is the same as used in a real OR. The HPS is anesthetized using a regular anesthesia machine. Many of the monitor instruments are also real and stimulated by physiological-like signals. The ECG, for example, is obtained from leads on the chest, from which an ECG-like signal originates. Some monitors, however, are fed directly with a signal from a model. An example is the pulse oximeter probe that is mounted on the patient's finger. It measures the absorption of light that changes with the amount of oxyhemoglobin, i.e. with the amount of oxygen in the blood. On the HPS a pulse oximeter probe is mounted on one of the fingers, but it is not used to measure the light absorption. Instead, the monitor is wired to a model, providing the correct signal.

The different models described above interact. As in real patients, changes in the cardiovascular system, for example, influence the pulmonary system.

full-scale patient simulator design considerations

In the development of full-scale patient simulators in general, four specific design levels can be identified [VanMeurs-97]. The *hardware* design includes the patient mannequin, exterior features, clinical signs representation, mechanical models, and computer systems. The *software* design includes the user interface, mathematical models, model parameters, communication protocol between computers, code structure, and programming language. The *curriculum* design includes the target learners, educational needs assessment, learning objectives, patient types, clinical scenarios, and formal evaluation methodology. The *exercise* design includes the number of participants, pace, modulation of severity, student-instructor interaction, and performance evaluation. Simulator hardware and software design decisions are usually made by simulator developers, while curriculum and exercise design decisions are made by clinical instructors.

An important decision in the software and hardware design levels is the implementation of the interface. The interface between the models and the user and real world equipment can be accomplished with either realistic physico-chemical interfaces, or with artificial interfaces. The use of real physico-chemical entities, such as electrical current for the ECG, and real gases for the simulated lung, add significant realism to full-scale simulation. It offers the advantage of an interface with standard, real-world medical equipment such as monitoring equipment and life support systems. Alternatives to physico-chemical interfaces are artificial interfaces. They can be realized electromechanically, connecting the computer, on which the mathematical software model runs, directly to the physiological monitor. Another possibility is to graphically emulate a display on a computer screen. If the monitored entity can be represented numerically, a minimal display can consist of only (alpha-)numerical data. A similar classification can be made for sensing therapeutic interventions.

The following section describes a draft curriculum design for a neurophysiological module for the HPS, established with the help of clinical instructors. This description is used as basis for the decisions in the hardware and software design, elaborated on in the following chapters.

3.3 Learning Objectives for a Neurophysiological Module

In cooperation with clinical instructors, the learning objectives for a neurophysiological module for the HPS were formulated. The instructors were not informed about implementation considerations, in order to get an objective idea about the educational needs. If in a later stage the implementations will limit the possibilities of some learning objectives, they have to be reconsidered, in cooperation with the instructors.

As a target audience anesthesia residents and EEG technicians were selected. Initially the learning objectives are limited to applications in the OR. Other application areas, such as sleep disorders, epilepsy, and MS, are not (yet) considered. Typically, neurophysiological monitoring in the OR is done by Ph.D. neurologists, EEG technicians supervised by an anesthesiologist, or EEG technicians supervised by a neurologist. Anesthesiologists doing neurophysiological monitoring in the OR are very rare, but an increasing interest is noticable, notably in Europe.

The handling of EEG monitoring equipment should be taught first, followed by the effects of anesthesia on the EEG and influences of surgery. All three elements of EEG monitoring should be taught separately before they can be combined. For this separate training a limited possibility of diagnoses should be implemented, in order to keep the focus on the specific learning objective. After the basic elements are taught independently, they can be combined in more complex trainings, such as clinical scenarios. Team training should be included at this stage, particularly the communication between the surgeon, the EEG technician, and the anesthesiologist.

Specific learning objectives in handling monitoring equipment are:

- understanding and experiencing the influence of technical factors on the obtained signal (e.g. filtering and equipment artifacts),
- recognizing and correcting artifacts (e.g. EMG, eye movement, ECG, loose electrode, mains interference, electrosurgery),
- evaluating recording quality, improving the quality if necessary.

Specific learning objectives in recognizing the effects of anesthesia are:

- understanding the influence of anesthetics on the central nervous system,
- understanding the concepts of analgesia, hypnosis, and amnesia as separate objectives of general anesthesia,

- illustrating the relationships between EEG recordings and more traditional monitoring modalities such as heart rate and blood pressure, and clinical signs.

An example of a simple simulation exercise in this context is the induction or maintenance of an anesthesia level with the EEG as a feedback signal.

Specific learning objectives concerning surgery-related influences on the EEG:

- recognizing injury as a result of surgery in an early stage to prevent or minimize further damage (e.g. general ischemia, strokes),
- recognizing and correcting compromising cardiovascular and respiratory situations, using EEG monitors in combination with other monitors,
- choosing an appropriate anesthetic agent that does not interfere with EEG monitoring.

Once these three categories of learning objectives are achieved, more complex objectives can be set:

- differentiating changes in monitored signals by: injury, pre-existing pathologic conditions, anesthetic agents, or equipment (mal-)functioning.

In order to realize these learning objectives a number of features has to be simulated. A raw EEG is the basis for educational simulation. A EEG simulation model should contain the effects of drugs on the EEG, the effects of general hypoxia and ischemia, and other influences, such as intercranial pressure (ICP), temperature, cerebral blood flow (CBF) and carbon dioxide pressure (CO_2).

The preference for a physico-chemical interface of the EEG model with the user and the equipment, as discussed in the previous section, implies that an (analog) electrical signal should be generated on (electrodes on) a head.

An EEG simulator can be implemented as a stand-alone simulator or as a part of the HPS. This choice is based on a consideration involving different learning objectives. Although most equipment related learning objectives can be realized with a stand-alone simulator, an EEG simulator as part of a full-scale simulator offers advantages. Equipment related learning objectives are better met in a full-scale environment and differential diagnosing can be based on realistic clinical signs in combination with the EEG. Therefore, a choice is made for the implementation of the EEG simulator as a module of the HPS. The learning objectives related to equipment, anesthesia, and surgery can then still be taught separately first.

Examples of clinical scenarios in which EEG monitoring is an essential part of the procedure are:

- carotid endarterectomy,
- cardiac anesthesia, especially deep hypothermic circulatory arrest,
- barbiturate coma,
- high risk operations such as brain aneurysm repair and brain tumor removal.

For these scenarios it is necessary to implement at least two EEG channels, and the effects of focal hypoxia and ischemia. Carotid endarterectomy is considered the preferred clinical scenario to implement, since it will have the biggest audience and the biggest impact for anesthesiologists not specializing in neuro anesthesia. It combines the raw EEG, anesthesia, and (possible) focal ischemia.

In the ideal case, the simulated signal would be indistinguishable from real EEGs. If indistinguishability is not obtained, at least important changes in the signal have to be sufficiently realistic to be recognizable and distinguishable from each other.

Initially the simulated patient is a young, healthy person, since research is mostly performed on volunteers of this category and results are published in the scientific literature. Different types of

4. EEG Model and Filter Design

Based on the learning objectives, described in the preceding chapter, a basic model for educational simulation of the EEG was developed by others. However, a comprehensive description of this model was still lacking. Part of this masters project was to formulate such a description, which is presented in the first section. Another part of the masters project was to carry out a formal design of the filters that form the signal generator of the basic model. This is described in the second section. The work described in this chapter is also presented in a scientific paper [DeBeer-97,I]. The simulation results at the end of this chapter are taken from this paper.

4.1 Existing Model Structure

There are two possible approaches for generation of the basic EEG signal. One of them is to simulate the EEG by simulating the underlying mechanisms, which requires a model for the brain's neuronal structure. The other approach is to simulate the resulting EEG-signal, for the greater part ignoring its origin. Although simulating the underlying mechanisms of the EEG is very interesting since it might yield a better insight into the organization and functioning of the brain, it is not the most computationally efficient approach. Previous studies describe models for the activity of small areas of the brain, for which a huge amount of development time and computer processing power is required [Lagerlund-88; Wilson-92; Jansen-95]. A real-time simulation of the EEG by means of such a brain model will therefore not be possible. This is the main argument for the choice to simulate the EEG signal components, rather than the underlying neurophysiologic phenomena.

Once this choice is made, there are two approaches to implement the automatic generation of the simulated patient's responses to therapeutic interventions: script-controlled or model-driven [VanMeurs-97]. A simulation script consists of a set of commands that cause the simulator to operate in a certain specified manner. It includes anticipated actions and interventions, such as surgery and administration of anesthetic drugs, and the simulated patient's response to them. Model-driven simulation requires a mathematical, electrical or mechanical model for the relationship between the input and output variables of the modeled process.

Scripts have the advantage of being explicit and unequivocal as to which responses to expect. Responses to events that are characterized by their occurrence and the time of occurrence are specially suited for script-controlled simulations.

Models can more easily generate responses to variables with a continuous range. In addition, models make it possible to take in to account a multitude of management options and interactions between different physiologic subsystems which would require an almost impossibly large number of states in a script-driven simulator.

Previous studies on EEG simulation use a script-like approach, in which prerecorded EEG samples, obtained from real patients in various clinical circumstances and settings, are replayed [Bashkaran-93]. The situations that can be simulated are limited by the availability of prerecorded samples. It is impossible to store EEG-samples resulting from every possible combination of therapeutic variables and patient types. A model-driven EEG simulator allows the combined effects of multiple variables (such as drug levels, oxygen saturation and blood pressure) to be considered simultaneously and facilitates simulating the EEG effects of continuous changes in these variables. The use of a model instead of real human EEGs requires a validation of the resulting signal on grounds of recognizability and usability for educational purposes (see chapter 3 on education).

EEG simulator

The above considerations led to the EEG signal simulation model as depicted in figure 4.1.

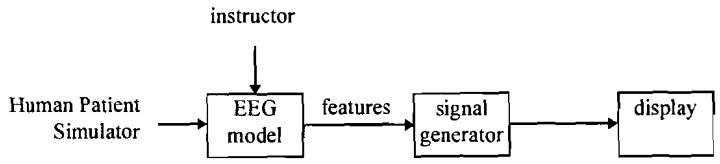

Figure 4.1: General structure of the EEG simulator

The EEG model generates the features that have to be included in the simulated EEG. The generation of the features will be based on variables that are calculated by other parts of the Human Patient Simulator or the parameters that are set by the instructor. The signal generator produces a digital EEG, reflecting the features specified by the EEG model. In order to display the simulated EEG, a standard hardware monitor or an emulated software monitor can be used.

Each of the components of the EEG simulator will be described in more detail below.

EEG model

A more detailed illustration of the intended EEG model integration in the HPS is given in figure 4.2. The simulated patient's characteristics (such as age and weight), pathology (diseases that influence the patient's heart functioning) and mental status (stress) will be set by the instructor before the simulation commences. During the simulation the instructor decides when events such as surgical procedures and severe blood loss take place. Other parts of the Human Patient Simulator continuously provide the variables that influence the EEG (such as drug effector site concentration (see chapter 5), arterial blood pressure, oxygen and carbon dioxide partial pressures, and temperature).

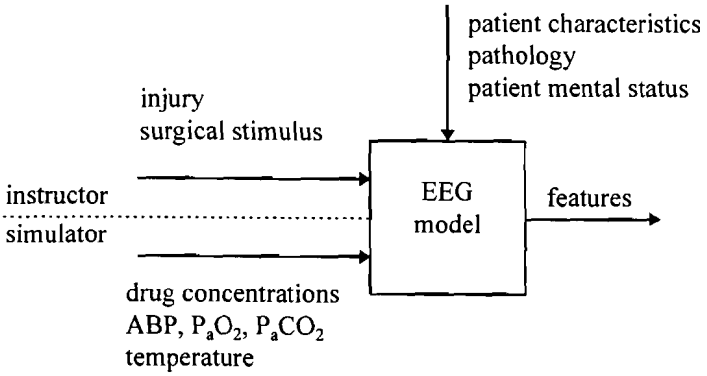

Figure 4.2: EEG model

An important decision for the EEG simulation is which features of the EEG signal are to be incorporated. This depends on: (1) which features are necessary for educational purposes, (2) the possibility to generate an EEG with those features, and (3) the availability of literature about the relations between the different independent variables and the features. The choice of features will be treated in section 4.2, the dependency of these features on anesthetic concentrations in section 5.2.

signal generator

The implementation of the signal generator is described in detail in [DeBeer-97,I] and illustrated in figure 4.3.

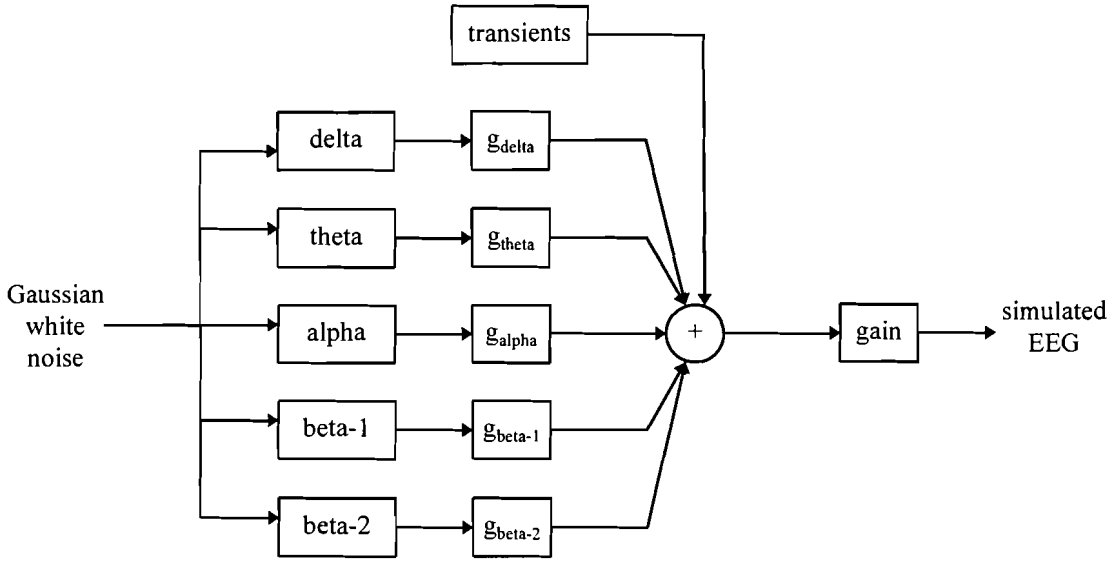

Figure 4.3: Implementation of the EEG generator.

Since the human spontaneous EEG resembles a stationary Gaussian signal, the EEG signal generator is based on linearly filtered, normally distributed white noise. The noise is filtered in five distinct frequency bands, corresponding to the conventional EEG frequency bands (see chapter 2.2). The frequency range of the resulting EEG is limited to 30 Hz., which should be sufficient when the EEGs of anesthesia patients are simulated. The division of the signal into five bands makes it possible to independently vary the power or amplitude of the EEG signal in each of the bands. Burst suppression patterns can be simulated by manipulating the overall gain. One way of adding transients or artifacts to the EEG is shown in figure 4.3. It may become necessary to extend the maximum generated frequency from 30 to 70 Hz, if the simulator is extended with other application areas such as sleep EEGs. In order not to exclude extensions of the model towards these higher frequencies, the sampling frequency is set at 256 Hz, which fulfills the Nyquist sampling theorem and is used in existing EEG monitoring equipment.

display

Using microvolt signals on electrodes attached to a mannequin head and a real EEG monitor to display simulator output offers the advantage of easy inclusion of a number of equipment related learning objectives, such as filter settings and artifact rejection, and will be more realistic than an emulated monitor [chapter 3 of this thesis, VanMeurs-97]. Therefore, the final implementation of the simulator is directed towards a real monitor. A (simple) emulated monitor is implemented for software and model testing during the development of the simulator.

The digital simulated EEG signal is interfaced to electrodes on a mannequin head. The signal passes a D/A converter and an attenuator, in order to obtain an analog signal with a realistic amplitude at the electrodes.

4.2 Filter Design for the Signal Generation Model

Van den Bosch and Van der Klauw [VandenBosch-94] describe modeling in a compact way: "It is the essence of the art of modeling to select only those characteristics, among the many available, which are necessary and sufficient to describe the process accurately enough according to the objectives of the modeler." A careful consideration of the question which inputs and outputs of a process need to be included in the model can influence the process of modeling very much. Including too many characteristics can result in an unnecessary complex model or unnecessary complex estimation of the model's parameters, whereas leaving out essential characteristics will make the model useless. Choosing a correct representation of the sufficient and necessary characteristics is important as well.

There are different types of models. Depending on the nature of the process the model will be a white or black box model or an intermediate form, called a gray box model. A white box model is derived by deduction only, based on the underlying physical laws and known parameters of the modeled process. Other processes, for which almost no prior information is available, are modeled by deriving a relationship between measured input and output data of the actual process. These models are called black box models. Gray box models describe those processes of which some underlying physical laws can be applied to arrive at a model, without knowing all the parameters of that model.

In case of black and gray box modeling the parameters of the model have to be estimated. An experiment has to be designed to obtain the required input-output data or data has to be extracted from scientific literature.

Parameter estimation brings about the necessity for validation of the model through simulation. The results of the simulation have to be validated with respect to new input-output data of the actual process. The validation can result in a change of the estimated parameters, but can also lead to changes of the model structure or even of the selected characteristics. Validation through simulation has to take place until a satisfying model with correct parameter values is found. [VandenBosch-94]

signal generation model

The EEG signal generation model of figure 4.3 is based on the observation that anesthesiologists and the anesthesia literature mainly describe the EEG by describing the amplitude or power of the spectrum in the different bands. Based on the model structure described in section 4.1, a decision has to be made which of its characteristics need to be variable and which can be fixed. The characteristics are the overall gain, the five independent band gains and the shape of the frequency spectra of the band filters. A real EEG spectrum shows peaks that are moving in the frequency domain with time, and peaks that change in width and in amplitude [Pichlmayr-85]. Therefore, both the band gains and the filter frequency spectra need to be variable in order to simulate an EEG spectrum that is indistinguishable from a real spectrum. For the purpose of educational simulation of the EEG, as discussed in chapter 3, recognizability of the features of the time signal, rather than indistinguishability of the spectrum or time signal is required. In that case the necessary and sufficient number of variable characteristics needs to be determined.

Initially the characteristics used by anesthesiologists, i.e., the amplitudes of the different frequency bands, are assumed to be sufficient to simulate an EEG for educational purposes. Therefore, these are taken as the only variable characteristics for the model. Leaving the gains variable and fixing the shape of the filters will be sufficient to simulate these characteristics. Since a validation of the simulated EEG in the time domain will have to prove whether leaving only the gains variable is sufficient, the possibility to implement a variable frequency transfer shape will be left open.

The final shape of the frequency spectrum of the simulated EEG is fully determined by the band filters since the frequency spectrum of a Gaussian white noise source is flat. For example, the frequency spectrum of the signal that results from filtering in the delta band will be the same as the delta filter's frequency transfer spectrum.

The EEG signal generator is based on the assumption that a time signal resulting from a filtering process will resemble another time signal (e.g., a real EEG) when the output spectrum of the applied filter resembles the spectrum of that other signal. Therefore, the filters will be designed on the resemblance of their frequency spectra with representative real human spectra found in [Pichlmayr-85]. If the shape of the filter frequency transfer needs to become variable, these fixed frequency spectra can be used as a starting point.

For filter design purposes the real EEG's frequency bands were parameterized as indicated in figure 4.4. The parameters are (1) the center frequency and (2) the bandwidth, which is defined as the frequency range between the -3dB (50%) points. Considerations in choosing this parameterization were the availability of data concerning these parameters in different situations, and the requirement that the parameterization should reflect the essential elements of the EEG spectral peaks.

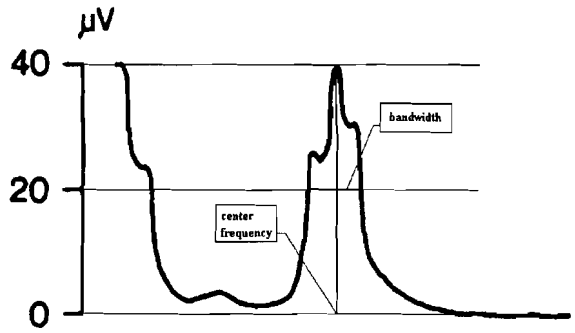

Figure 4.4: Illustration of the EEG peak parameterization

The real human EEGs are described with the help of this representation. For each band a representative peak was parametrized using the above method. The bandwidths and center frequencies obtained in this fashion can be found in table 4.1.

Table 4.1: Bandwidths (at the -3 dB points) and center frequencies of actual EEG spectra.

	Bandwidth (Hz)	Center frequency (Hz)
delta	2.1	2.0
theta	1.9	5.3
alpha	2.1	10.2
beta-1	4.0	14.0
beta-2	4.3	23.6

This parametric description of the desired filter frequency transfer forms the basis of the design of the band filters. The required precision and several additional requirements are formulated in the next section, followed by the filter design method and the calculation of the filter coefficients. With

these filter coefficients three different EEG signals (each characterized by a set of gains) are simulated. The results are evaluated for their realism by clinicians.

The supplementary requirements are divided into three categories: requirements concerning the EEG signal and frequency spectra, anticipated future extensions, and implementation considerations.

signal and frequency spectra requirements

The (fixed) filter frequency transfers need to reflect the parameterization of the parameters in table 4.1 with a precision of 0.1 Hz. This desired precision reflects the limits of the measurements underlying the parameterization method. In order to prevent too much overlap of the main lobes of the frequency spectrum of each filter with the side lobes of adjacent filters, the maximum amplitude of side lobes is limited to 10% of the amplitude of the main peak of the same frequency spectrum. This criterion of 10% is chosen to be consistent with the accuracy with which the desired EEG band amplitudes can be determined.

Linear phase is set as a requirement, to avoid distortion of the basic signal by filters for different channels. The current model generates one channel, but will be extended in the near future towards a multi-channel model. The different channels of an EEG show a strong correlation, illustrated by similar waves that occur simultaneously in the different channels. Although it is not yet known how the extension towards a multi-channel EEG will be implemented, this correlation should not be affected by distortion due to non-linear phase.

anticipated future requirements

Anticipating a possible future need to implement the filter frequency transfer shapes as variables, the filter coefficients should be the result of an analytically solvable calculation, based on the filter characteristics. If such a calculation is not possible, a look-up table can be used as an alternative. Such a table should give values for the filter coefficients (or derived parameters allowing to analytically calculate the filter coefficients) for different combinations of bandwidth and center frequency.

implementation requirements

The EEG has to be generated in real-time on a PC 486-66 Hz, implying that the number of calculations needed to generate the signal must be limited. The number of necessary calculations will increase and might even increase drastically if more channels are implemented. It is not yet known how many channels will be generated nor how these extra channels will be implemented, but it might be necessary to use separate filters for each channel, causing an increase in calculations. In order to anticipate this increase in number of calculations, a low number of filter coefficients is preferred.

The model of figure 4.3 requires filters with non-complex (real-valued) coefficients, since a real signal has to be generated. The amplitude at the center frequencies after the first band filters will be scaled to one, so that the final amplitude at the center frequencies will be determined solely by the gains. The scaling is a valid course of action since Fourier transformation is a linear process, which means that multiplication of the coefficients with a constant value will only change the amplitude and not the shape of the frequency spectrum.

filter selection and implementation

The two basic filter classes are Finite Impulse Response (FIR) and Infinite Impulse Response (IIR) filters. Although in designing IIR filters it is usually possible to approximate a desired magnitude response in an efficient way, the resulting phase is generally not linear, resulting in distortion of the (EEG) signal in the time domain. Since in FIR filter design linear phase can be enforced by using a symmetric impulse response, this class of filters is preferred over IIR filters.

Some functions such as the sinc, $sinc^2$ and some of the functions associated with spectra belonging to window functions in the time domain (see figure 4.5) seem suited for the desired filters, since they can be adapted to fit the parameterized description of the EEG bands. It will be shown, however, that these functions do not meet all the requirements.

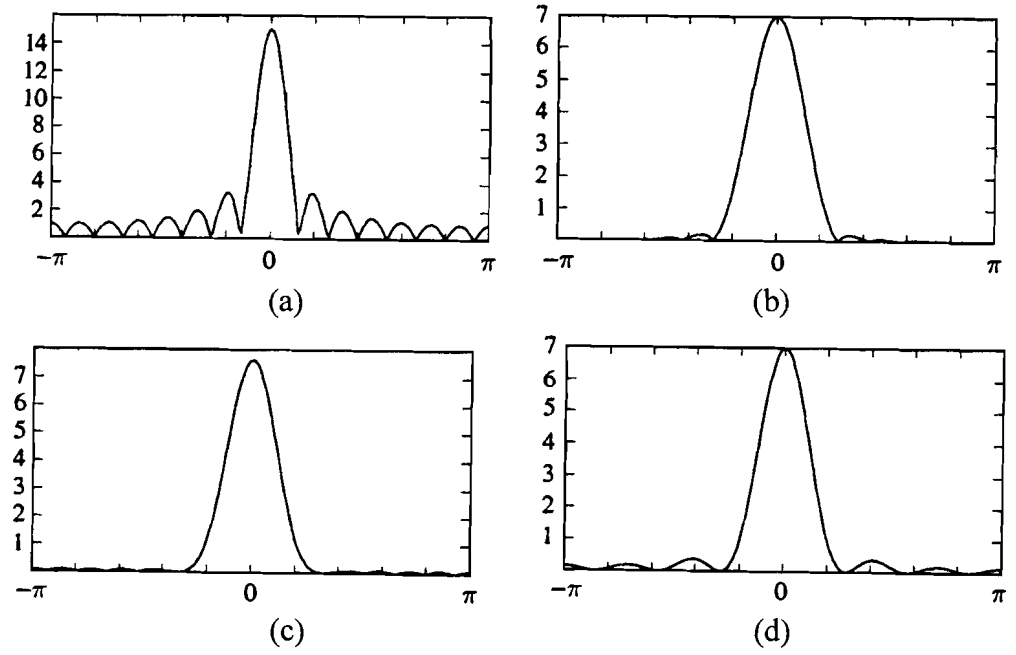

Figure 4.5: Frequency spectra of time domain window functions: (a) rectangular (b) Hann (c) Hamming (d) Bartlett. On the horizontal axes the relative frequency is given, on the vertical axes the amplitude of the frequency spectrum.

These functions (sinc, $sinc^2$, and the functions belonging to the spectra of the window functions) in the frequency domain can be transformed, applying Fourier transformation, to real-valued functions in the time domain. These functions could thus be used as (real-valued) filter coefficients. However, these frequency functions are symmetric around zero and need to be shifted in frequency in order to represent EEG peaks. This shift in frequency is accompanied by a multiplication with a complex number in the time-domain, resulting in complex filter coefficients. The frequency shifted Fourier transform of the standard Fourier pair

$$x[n] \leftrightarrow X\left(e^{j\omega}\right) \tag{4.1}$$

is

$$e^{j\omega_0 n}x[n] \leftrightarrow X\left(e^{j(\omega-\omega_0)}\right), \tag{4.2}$$

making these functions useless for the purpose of EEG simulation.

In FIR filter design, a commonly used method is windowing [Oppenheim-89]. Starting with an ideal frequency transfer spectrum, inverse Fourier transformation is applied in order to find the matching ideal impulse response. Since this is usually an infinite impulse response, a finite-length window in the time-domain is applied in order to truncate this response. Some of the more often used windows are the rectangular, Bartlett, Hann, Hamming and Blackman windows (see figure 4.6).

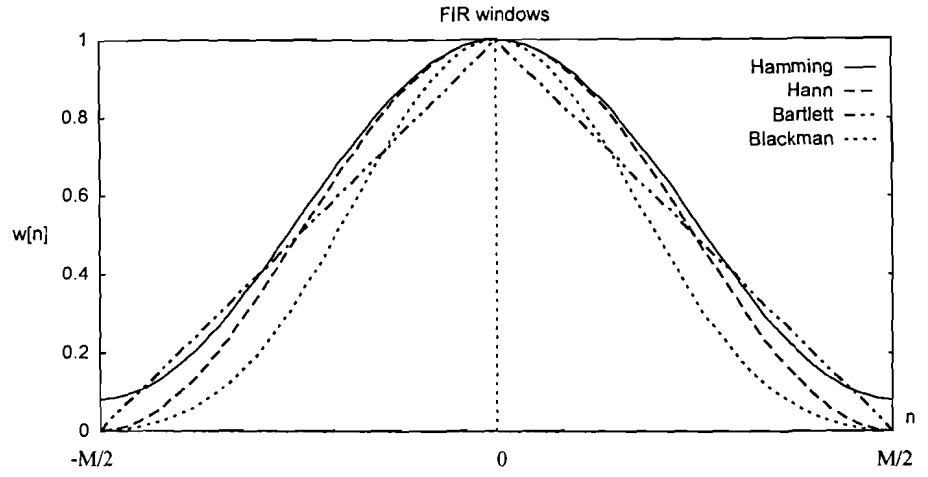

Figure 4.6: FIR windows of width M

In the frequency domain, the effect of windowing is that the ideal spectrum is convolved with the Fourier transform of the applied window.

The filter coefficients of an FIR filter applying a window are real-valued. The shape of the filter's frequency spectrum is a function of the cut-off frequencies and the width of the window (the number of filter elements). Increasing the width of the window will result in a frequency transfer spectrum that better resembles the ideal frequency transfer spectrum. This implies, amongst others, that the side lobe amplitude decreases.

An ideal bandpass filter, combined with a window of appropriate length, results in a frequency transfer function that is characterized by peaks that resemble the shape of EEG peaks. The frequency spectrum of an ideal bandpass filter is:

$$H_d(e^{j\omega}) = \begin{cases} 1 & (a\pi \le |\omega| \le b\pi) \\ 0 & (|\omega| < a\pi, b\pi < |\omega|) \end{cases} \qquad (4.3)$$

where $a\pi$ and $b\pi$ are the relative cut-off frequencies. For b=1 the above definition describes an ideal highpass filter, for a=0 an ideal lowpass filter. The filter coefficients of the ideal bandpass filter are calculated by Fourier transforming this frequency spectrum:

$$h_d(n) = \frac{1}{2\pi}\int_{-\pi}^{\pi} H_d(e^{j\omega})e^{j\omega n}d\omega = \frac{1}{2\pi}\left[\int_{-b\pi}^{-a\pi} e^{j\omega n}d\omega + \int_{a\pi}^{b\pi} e^{j\omega n}d\omega\right] = \frac{\sin b\pi n - \sin a\pi n}{\pi n} \qquad (4.4)$$

Applying a window in order to decrease the filter length alters the ideal impulse response into the final impulse response (or filter coefficients) by multiplying each coefficient with a window coefficient:

$$h(n) = w(n)h_d(n) = w(n)\frac{\sin b\pi n - \sin a\pi n}{\pi n} \tag{4.5}$$

Using this truncated impulse response, the final filter transfer spectrum is given by:

$$H(e^{j\omega}) = \sum_{n=-\infty}^{\infty} h(n)e^{-j\omega n} = \sum_{n=-\frac{N}{2}}^{\frac{N}{2}} w(n)\frac{\sin b\pi n - \sin a\pi n}{\pi n}e^{-j\omega n} =$$

$$= w(0)(b-a) + \sum_{n=1}^{\frac{N}{2}} 2w(n)\frac{\sin b\pi n - \sin a\pi n}{\pi n}\cos\omega n \tag{4.6}$$

The window and the values for a, b, and N determine the shape of the final filter frequency spectrum. Since they cannot be obtained directly from literature, the values for these parameters have to be found that fulfill the parametrization into bandwidth and center frequency and the other filter requirements.

filter parameter estimation

The passband of the filter frequency spectrum of equation 4 will be symmetrical around the center frequency ω_c, which is equal to the middle of the ideal bandpass filter or $(a+b)\pi/2$. Thus the desired center frequency is determined by the value for (a+b).

For bands of the ideal passband filters that are narrow in comparison with the sampling frequency, which is the case in this application, the resulting actual filter bandwidth will be larger than the ideal passband width $(b-a)\pi$. Decreasing (b-a) for a given number of coefficients will result in a lower actual filter bandwidth. However, there is a lower limit for (b-a), below which decreasing (b-a) will not result in a further decrease of the filter bandwidth. Using a value for (b-a) well below this limit, the actual filter bandwidth can be further manipulated by manipulating the number of filter coefficients N+1. Increasing the number of coefficients results in a better approximation of the ideal bandpass filter, and consequently a smaller bandwidth of the resulting filter frequency spectrum, while decreasing N will result in a larger bandwidth. This procedure results in a pair of values for (b-a) and N that realizes the desired bandwidth at a small value of N.

The amplitude of the side lobes can be manipulated by the choice of window. For each band and for different windows, a pair of (b-a) and N, derived with the procedure described above, can be found. For the bandwidths necessary for the present application, the Hann window was found to be the window meeting the side lobes requirement with the lowest number of filter elements. The equation describing the Hann window is:

$$w[n] = \begin{cases} 0.5 + 0.5\cos(2\pi n / M) & -M/2 \le n \le M/2 \\ 0 & \text{otherwise} \end{cases} \tag{4.7}$$

The final filter coefficients and the final frequency spectrum (see formula (4)), applying a Hann window are:

$$h(n) = (0.5 - 0.5\cos(2\pi\frac{n-\frac{N}{2}}{N}))\frac{\sin b\pi n - \sin a\pi n}{\pi n} \qquad \text{for } -\frac{N}{2} \le n \le \frac{N}{2}$$

$$H(e^{j\omega}) = (b-a) + \sum_{n=1}^{\frac{N}{2}}\left(1 - \cos(2\pi\frac{n-\frac{N}{2}}{N})\right)\frac{\sin b\pi n - \sin a\pi n}{\pi n}\cos\omega n \tag{4.8}$$

Table 4.2 shows the resulting values for a, b, and N for the Hann window.

Table 4.2 estimates for the parameters f_a, f_b, corresponding relative frequencies a and b, and estimates for N for calculation of the filter coefficients. F_{samp} = 256 Hz.

	f_a (Hz)	f_b (Hz)	a	b	N
delta	1.99	2.01	.0155	.0157	240
theta	5.29	5.31	.0413	.0415	260
alpha	10.19	10.21	.0796	.0798	240
beta-1	13.9	14.1	.109	.110	124
beta-2	23.5	23.7	.184	.185	140

simulation results

Three typical EEGs (awake, isoflurane, and halothane EEG) are described in [Yli-Hankala-90]. The values for the amplitude per band given in that paper were implemented in the model. The resulting EEGs are compared with the EEGs as shown in [Yli-Hankala-90]. Three anesthesiologists with EEG monitoring experience compared the simulated and the original EEGs for these three situations. The signals were presented as shown in figure 4.7.

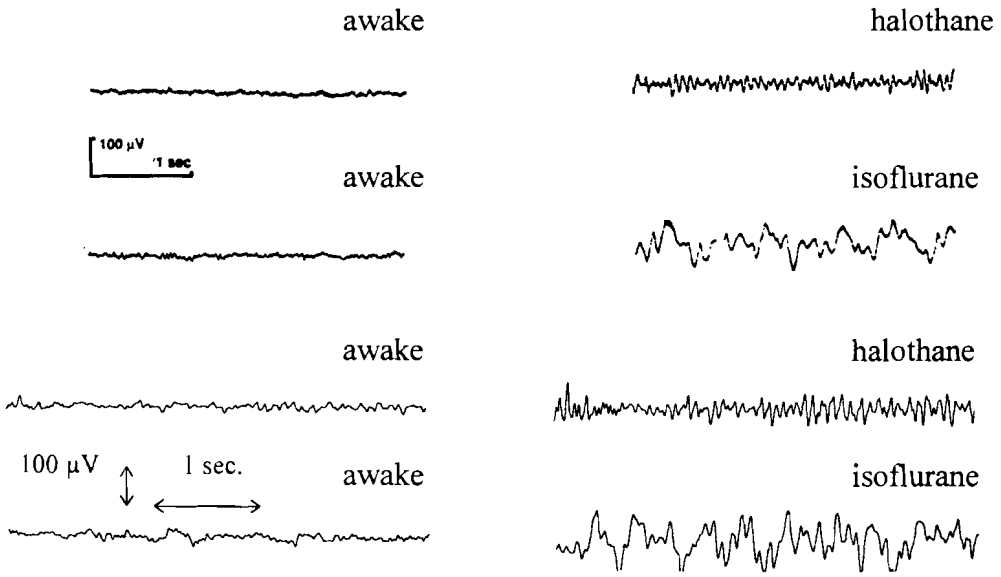

Figure 4.7: Comparison of actual recorded EEGs (upper graph, from Yli-Hankala [1990], permission granted by Munksgaard International Publishers Ltd., Copenhagen, Denmark) and simulated EEGs for three different sets of the band gains.

The experts were asked the following questions:

- In your opinion, does the simulated signal bear enough resemblance to the actual recording in order to be used for educational simulation?

- Do you think the simulated EEG signals can be considered typical for an awake, isoflurane and a halothane EEG?

All three experts answered positively to these questions. One expert could give some minor differences between the actual and the simulated EEGs. The awake baseline looks like a drowsy EEG, since there is a little too much activity of slow frequencies. The peaks in the isoflorane EEG are too sharp.

5. Modeling of Drug Effects on the EEG

For the described EEG model to gain full educational applicability, it also has to simulate dynamic, notably the influence of anesthetic drugs on the EEG. Pharmacokinetic and pharmacodynamic modeling is a rapidly evolving field of research. Therefore, part of the masters project was to summarize the current insights from an engineering perspective. This information is used as a basis for describing the existing drug effect model of the EEG simulator, which is the topic of the last section.

5.1 Pharmacokinetic models

The time-course and magnitude of the effect of a drug on the EEG can be explained by a combination of two processes. Before taking an effect, the drug first has to be distributed in the body and to the brain. When present at the brain, the drug will have its effect on e.g. receptors, changing the characteristics of the EEG. The process of distribution and elimination of drugs, including transport to different effector sites is called pharmacokinetics. The study of the relation between the effector site concentration and the effect is called pharmacodynamics. Based on [Hull-79], [Nikkelen-95], and discussions with Dr. W.L. van Meurs [VanMeurs-PC-97] a description of the current status of pharmacokinetics and pharmacodynamics is made.

pharmacokinetics

When a drug is administered to a patient, the onset and duration of its effect depend upon the rate of absorption into the bloodstream, distribution to various organs, tissue binding, access to those tissues where the pharmacological effect takes place, interaction with receptor sites, and elimination by various routes.

Absorption is the process of drug delivery to the plasma. It includes a number of physical processes such as route of administration, ionization, transport across membranes, and protein binding. These processes influence the amount of active drug reaching the plasma in the tissue where the effect takes place, the so-called effector site. The rate of absorption plays an essential role in the time course of a drug effect after drug administration and is thus an important consideration in determining drug dosages.

Distribution describes the transport of a drug to all parts of the body, and notably to the effector site. It is the reversible transfer of a drug from one location to another and involves the circulation through the bloodstream, movement across lipid membranes and capillary walls, and movement between active and inactive binding sites in different tissues of the body. The distribution is influenced by the characteristics of the drug, the cardiac output, and the blood flow to the various organs and tissues. Organs with a high perfusion such as the heart, brain, kidney, and liver, receive drugs rapidly after administration. Muscles are less perfused at rest and will receive drugs slower, and fat, which is hardly perfused, will receive drugs even slower. In peripheral tissues, such as fat, drug amounts may become very high because the drug binds to the tissue or dissolves in it. In particular during long durations of drug administration, the amount of drug accumulated in fat may become very high.

Elimination or clearance is the irreversible process of removal of drugs in their active form from the body. Elimination takes place through renal clearance (by the kidneys), hepatobiliary metabolism

(by the liver), and pulmonary excretion (via the lungs). Other routes of elimination are saliva, sweat, breast milk, and tears. The most important form of elimination concerning pharmacokinetics is metabolism. The rate of metabolism of most drugs is determined by the concentration of the drug at the metabolic site.

exponential model

Since the body consists of a high number of tissue zones, each with its unique perfusion, drug solubility, drug binding affinity, etc., a white box mathematical description (see section 4.2) of the pharmacokinetic properties of a drug will be complex. In order to be able to make a model for which the (patient dependent) parameters can be derived from a reasonable amount of measured data, major simplifications need to be made.

After administration of a drug bolus, the plasma drug concentration quickly rises to a certain level. The concentration then decreases as time continues.

This time response of the plasma concentration after a bolus can often be approximated with a summation of exponentials with different amplitudes (A_i) and hybrid time constants (λ_i):

$$c_{pl}(t) \cong \frac{D}{V_1} \sum_{i=1}^{n} A_i e^{-\lambda_i t} \qquad (5.1)$$

where D is the administered dose, V1 is the apparent volume of distribution, and n is the order of the kinetics. Typical values for the plasma drug concentration are of the order of mg/l or μg/l. See figure 5.1 for an example of a plasma concentration, modeled as a summation of exponentials. (The effector site concentration will be treated later in this section). The parameters of this equation can be extracted from the time response of the plasma drug concentration after bolus administration.

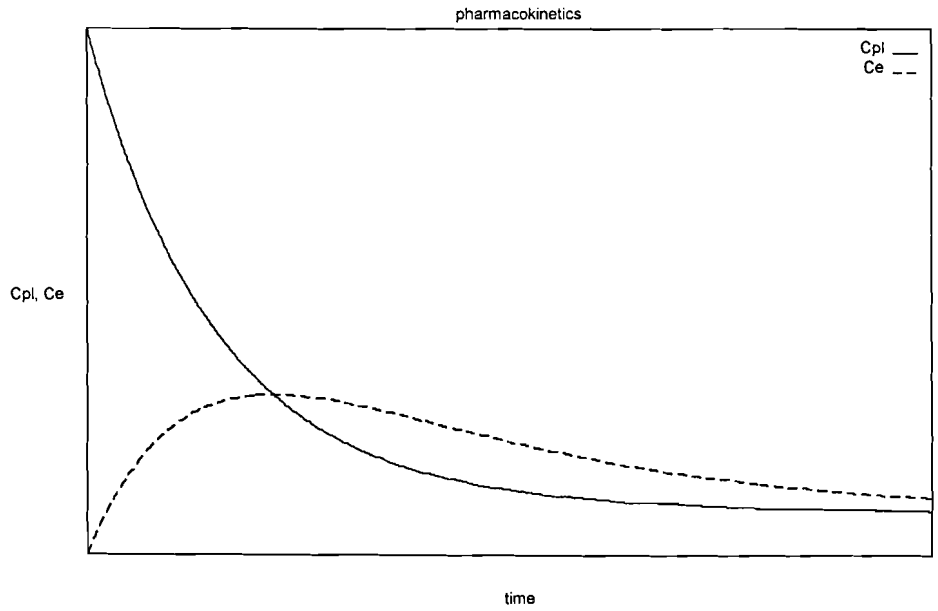

Figure 5.1: Time responses of plasma and effector site drug concentrations (c_{pl} and c_e) after administration of a bolus.

compartment model

The pharmacokinetic processes underlying the plasma concentration curve are often interpreted by a compartment model. This model describes the absorption, distribution, and elimination taking place in one or more compartments with uniform characteristics of distribution and transport. These compartment model parameters can be directly derived from the parameters of equation 5.1. A two-compartment pharmacokinetic model is depicted in figure 5.2.

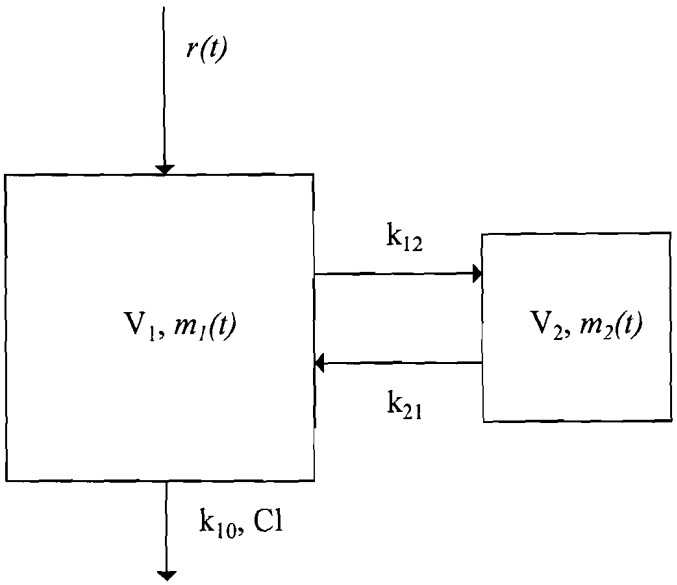

Figure 5.2: Schematic representation of a two compartment pharmacokinetic model. See text for an explanation of used abbreviations.

Although this compartment model is a mathematical description of the plasma concentration as a function of administration of drugs, it is possible to roughly imagine what processes take place in which compartments. The first or central compartment mainly represents the drugs in the highly perfused tissues such as the heart, brain, kidneys, and liver. The second or peripheral compartment represents storage in other tissues. Some drugs require a third compartment in order to correctly describe its kinetics.

Drugs enter the central compartment directly and are distributed from the central to the other compartments. The amount of (intravenously) administered drug is represented by r(t) and can consists of a bolus (represented mathematically with a delta-function with an amplitude equal to the dose) or an infusion rate. The rate of distribution k_{ij} (typically given in min^{-1}, determines the velocity of drug transport from compartment i to j. Elimination is supposed to only take place from the central compartment and is represented by k_{10}.

Compartment models describe the change of drug mass over time:

$$\frac{dm_1(t)}{dt} = -(k_{10} + k_{12})m_1(t) + k_{21}m_2(t) + r(t) \qquad (5.2)$$

$$\frac{dm_2(t)}{dt} = k_{12}m_1(t) - k_{21}m_2(t) \qquad (5.3)$$

where m_i is the mass of the drug present in compartment i.

The concentrations in the different compartments are calculated by dividing the masses resulting from equations 5.2 and 5.3 by their respective volumes of distribution (V_i). Since the only measurable entity is the plasma concentration, only the concentration of the drugs in the central compartment is of interest:

$$c_1(t) = \frac{m_1(t)}{V_1} \tag{5.4}$$

clinical model

A third way of modeling of pharmacokinetics often found in the literature is termed "clinical pharmacokinetics". It is represented by measurable entities, such as drug concentration half times. This model is not described in detail here, but it is mentioned since clinicians often refer to parameters of this model when describing pharmacokinetics. One of the clinical parameters, the elimination clearance of a drug, is given by the product of the elimination rate constant and the volume of the central compartment (equation 5.5).

$$Cl = k_{10}V_1 \tag{5.5}$$

This clearance indicates the sum of all elimination pathways. If the clearance or the rate constant is given, the other can be calculated using this equation.

apparent effector site concentration

The effect of a drug is modeled by a static relationship between the durg concentration in a hypothetical effector site of negligible volume and a measurable effect. A first order concentration driven process determines how the effector site concentration depends on the plasma concentration:

$$\frac{dc_e(t)}{dt} = k_{e0}\left(c_1(t) - c_e(t)\right) \tag{5.6}$$

where k_{e0} is the equilibration time constant.

Because of the hypothetical nature of the effecor site, its concentration is called an apparent concentration. It is defined as the plasma concentration in a steady state situation that results in the same effect.

k_{e0} can be calculated from the time responses of the effect and the plasma concentrations [Sheiner-79], [VanMeurs-97]. For each effector site a different effector site concentration can be calculated, using a different k_{e0}.

The application of equations 5.2, 5.3, 5.4, and 5.6 on a bolus of a drug typically results in the plasma and effector site concentration time responses as shown in figure 5.1.

5.2 Modeling Drug Effects on the EEG

The EEG characteristics are modeled for different types of anesthetic drugs. The description of the drug effect model in this section can be found in [DeBeer,97,II].

pharmacodynamics

Pharmacodynamics describe the relation between effector site drug concentration and the drug effect. At the effector site the drug acts on excitable membrane proteins such as receptors, ion channels, and ion pumps to initiate its effect. Many effects can be described with a sigmoide function of the effector site concentration (figure 5.3) using a general form of the Hill equation [Holford-81]:

$$Effect(t) = E_0 + (E_{max} - E_0)\frac{c_e(t)^\gamma}{c_e(t)^\gamma + (EC_{50})^\gamma} \qquad (5.7)$$

E_0 is the effect when no drug is present, E_{max} is the maximum possible effect caused by the drug, EC_{50} is the drug concentration associated with an effect half the difference between E_{max} and E_0, γ is the Hill-coefficient, determining the slope of the sigmoide.

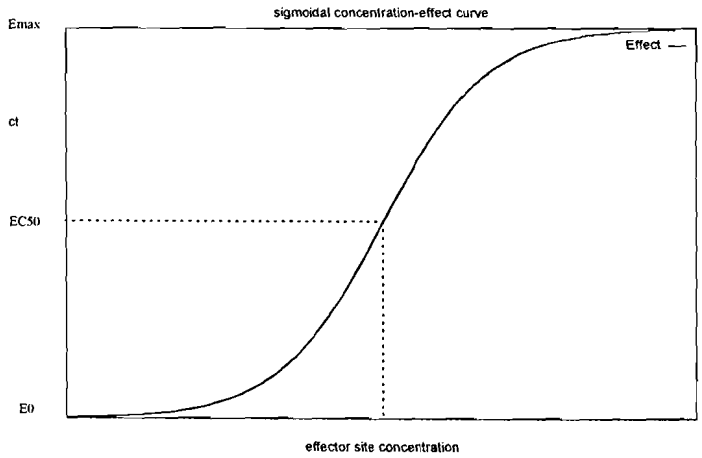

Figure 5.3: Sigmoidal effector site concentration-effect curve

This sigmoidal curve or concentration-effect curves of a different shape can also be approximated with a piecewise linear description.

modeling the spectral amplitudes

The input variables of the EEG model described in section 4.1 considered in this report are the effector site concentrations of various drugs. The variable output features of the EEG model, the amplitudes of the signals in the conventional frequency bands, have to be dynamically modeled as a function of this input variable. The relation between the effector site drug concentration and the drug effect is called a pharmacodynamic relation.

For one drug, each band gain is modeled as a piece-wise linear function of the effector site concentration. An example of such a function is:

$$g(c_e) = g(0) + S \bullet a(c_e) \tag{5.8}$$

with

$$a(c_e) = \begin{cases} 0 & c_e < c_{e,min} \\ c_e - c_{e,min} & c_{e,min} \le c_e \le c_{e,max} \\ c_{e,max} - c_{e,min} & c_e > c_{e,max} \end{cases} \tag{5.9}$$

For each gain the values for the parameters g(0), S, $c_{e,min}$, and $c_{e,max}$ can be different. The model belonging to this equation assumes the effect of an anesthetic drug eith effector site concentration can be described as an absolute effect added to a baseline effect g(0). The model also assumes that the gain changes linearly with changing anesthetic concentrations, and that the slope of this change is S_k. For volatile anesthetics, the effector site concentration is replaced by effector site partial pressure.

An extension of this function allows the effect of a drug to have different slopes at different intervals of the effector site concentration, maintaining a linearity at each of these intervals:

$$g(c_e) = g(0) + \sum_{k=1}^{K_m} S_k \bullet a_k(c_e) \tag{5.10}$$

with

$$a_k(c_e) = \begin{cases} 0 & c_e < c_{e,k,min} \\ c_e - c_{e,k,min} & c_{e,k,min} \le c_e \le c_{e,k,max} \\ c_{e,k,max} - c_{e,k,min} & c_e > c_{e,k,max} \end{cases} \tag{5.11}$$

The number of linear intervals is K_m, which can be different for different drugs.

Figure 5.4 gives an example of the effect of one drug (thiopental) on the delta gain. The piece-wise linear function for the delta gain is [DeBeer-97,II]:

$$g_\delta = g_\delta(0) + 25 \bullet activation_1(c_e) - 12 \bullet activation_2(c_e) \tag{5.12}$$

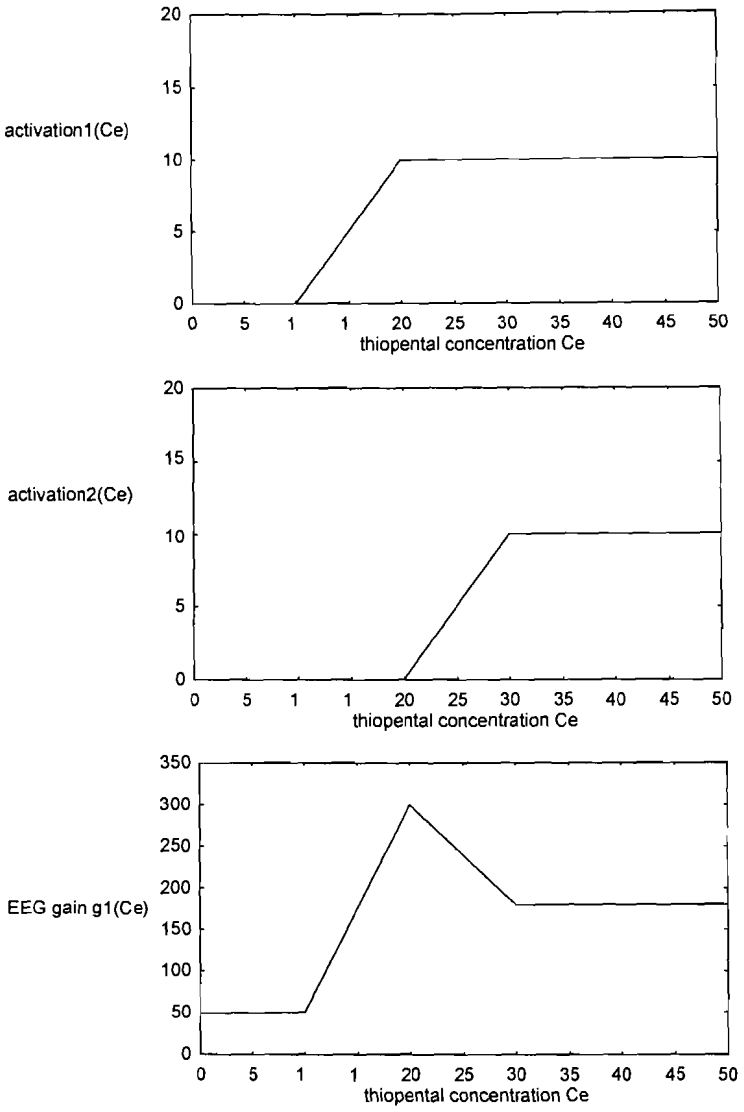

Figure 5.4: Piece-wise linear model of the effect of thiopental on the delta gain. Thiopental effector site concentrations in mg/l.

To include the effects of more than one drug, the effects of the drugs are assumed to be additive. This results in the description of each gain as a function of the effector site concentrations of M different drugs:

$$g(c_{e,1},c_{e,2},\ldots,c_{e,M}) = g(0,0,\ldots,0) + \sum_{m=1}^{M}\sum_{k=1}^{K_m} S_{k,m} \times a_{k,m}(c_{e,m}) \tag{5.13}$$

with

$$a_{k,m}(c_{e,m}) = \begin{cases} 0 & c_{e,m} < c_{e,m,k,min} \\ c_{e,m} - c_{e,m,k,min} & c_{e,m,k,min} \le c_{e,m} \le c_{e,m,k,max} \\ c_{e,m,k,max} - c_{e,m,k,min} & c_{e,m} > c_{e,m,k,max} \end{cases} \tag{5.14}$$

modeling burst suppression

Burst suppression can be characterized by a number of variables. The average suppression duration, the average burst duration, and the number of bursts (or silences) per minute are dependent quantities. If two are given, the third can be calculated.

With increasing anesthetic concentrations the suppression duration increases and the burst duration decreases. The durations are average values, the actual values vary around the average value.

Assuming the number of bursts per minute increases with increasing concentration, the variables APM (average number of periods per minute) and ASD (average suppression duration) are approximated with a linear function of the concentration.

$$ASD = S_1(c_e - c_{on}) \qquad c_e \geq c_{on} \tag{5.15}$$

$$APM = APM_0 + S_2(c_e - c_{on}) \qquad c_e \geq c_{on} \tag{5.16}$$

where S_1 and S_2 are constants, APM_0 is the initial number of periods per minute, ce is the effector site concentration, and c_{on} is the onset effector site concentration at which burst suppression starts to appear.

The ABD (average burst duration) is calculated, using the equation:

$$ABD = \frac{60}{APM} - ASD \qquad c_e \geq c_{on} \tag{5.17}$$

In order to prevent the signal from looking deterministic, the actual burst and suppression durations are varied around the desired values. Depending on the values of ASD and ABD it is determined in real-time whether the overall gain of the EEG simulation model (figure 4.3) should be set to 1 (burst) or 0 (suppression). The burst intervals are allowed to end every ΔT seconds with a probability p_b, the suppression periods every ΔT with a probability p_s, with

$$p_b = \frac{\Delta T}{ABD} \qquad p_s = \frac{\Delta T}{ASD} \tag{5.18}$$

The resulting intervals will vary in duration between zero and infinity, with average durations equal to ABD and ASD. The minimum value of the intervals is set at 0.5 seconds, to prevent two consecutive suppression or burst periods from merging. To smoothen the transition between burst and suppression periods (a burst cannot start with a value unequal to zero, or the signal would be discontinuous) the overall gain resulting from ASD and ABD is filtered with a first order lowpass filter.

Signal characteristics during burst periods are assumed to be the same with or without the occurrence of burst suppression, justifying the choice to only vary the overall gain in figure 4.3.

6. Critical Model Evaluation: Integration of Propofol

The number of drugs integrated in the EEG simulator is still limited. In order to enlarge the number of drugs, propofol is added to the model. The process of integration of propofol is used to critically evaluate the existing EEG model. Pharmacokinetic and pharmacodynamic parameters for propofol are extracted from the scientific literature and implemented in the existing model. Based on the simulation results of the effects of a propofol bolus, the model for the band gains is improved. Because the existing burst suppression model was inaccurate, a modified burst suppression model is implemented. The resulting new model is used to simulate the effects of the same propofol bolus. The resulting EEG is evaluated by EEG experts. The new burst suppression model, with parameters for propofol, is also evaluated by an EEG expert. From these evaluations, recommendations for further improvements of the existing EEG simulator resulted. The new burst suppression model is also described in [DeBeer-97,I] and [DeBeer-97,II].

6.1 The Effects of Propofol on the EEG

Propofol is an intravenously administered hypnotic agent and is mainly used to induce and maintain anesthesia. It is also used for single-dose intravenous anesthesia for brief procedures such as dental surgery, in surgery for patients who need pain relief and transient loss of consciousness to undergo local injection of anesthesia, and for sedation in intensive care units [Reddy-92]. It is known for its fast onset and swift recovery [Traast-95].

pharmacokinetics of propofol

Eventually, the EEG-simulation module will be integrated with the Human Patient Simulator. The values for effector site concentration will then be obtained from a different part of this HPS [VanMeurs-97,I]. For the moment the EEG model will be used as a stand alone simulator, which requires a pharmacokinetic model for the calculation of the effector site concentration of the implemented drugs.

For propofol a number of pharmacokinetic compartment models have been suggested, some suggest a two-, others a three compartment model [Schüttler-85], [Frenkel-95]. [Kirkpatrick-88] fitted a three-compartment model to most patients, but needed a two-compartment model to fit the propofol concentration curve of two elderly patients.

In [Kirkpatrick-88], together with the pharmacokinetic parameters, the time response of the blood propofol concentration after bolus administration is presented, which gives the possibility to validate the implementation of the pharmacokinetic model of the EEG simulator. For this reason the parameters for the compartment model are taken from [Kirkpatrick-88].

For a long time, [Schüttler-85] was the only source in scientific literature for a blood-brain equilibration half-life for propofol. With this half-life the parameter k_{e0} can be calculated to have the value 0.239 min^{-1} ($k_{e0} = \ln 2 / t_{1/2e}$). The effect measured in his study was the EEG's mean frequency. Recently [Billard-97] determined a k_{e0} of 0.27 min^{-1} for the effect on relative delta power, 0.21 min^{-1} for spectral edge frequency, and 0.20 min^{-1} for the bispectral index. These values are similar to those found in [Schüttler-85]. The values for the pharmacokinetic parameters of propofol are summarized in table 6.1. The average weight of the patients in [Kirkpatrick-88] was 61.8 kg.

Table 6.1: Propofol pharmacokinetic parameters.

V_1	26.3 (l)
k_{12}	$2.46 \cdot 10^{-1}$ (min^{-1})
k_{21}	$5.97 \cdot 10^{-2}$ (min^{-1})
k_{13}	$3.91 \cdot 10^{-2}$ (min^{-1})
k_{31}	$1.91 \cdot 10^{-3}$ (min^{-1})
k_{10}	$0.77 \cdot 10^{-1}$ (min^{-1})
k_{e0}	$2.4 \cdot 10^{-1}$ (min^{-1})

The effector site concentration, calculated with the model described in section 5.1 with the parameters given above, will be used as the basis for the modeling of the EEG signal generator band gains and burst suppression parameters.

modeling the band gains

As described in chapter 4, the EEG signal generator requires two kinds of slowly time-varying parameters: the gains of the different frequency bands and burst suppression characteristics. This section describes how propofol apparent effector site concentration affects the gains, the next section how it affects burst suppression.

An extensive literature search was performed in order to gather data about the relation between the appearance of the EEG and the propofol effector site concentration. The following articles were retained: [Kearse-89], [Kishimoto-95], [Mahla-92], [Reddy-92], [Seiffert-93], [Sneyd-94], [Suttmann-89], [Traast-95], [Veselis-92], and [Veselis-93].

These articles give two types of information on the relationship between the effector site concentration and the EEG: the dose and concentration dependent power in the conventional bands, and the qualitative changes in the appearance of the EEG time signal. The first decription is mainly used for estimation of model parameters, the second for evaluation of the resulting signal.

With rising apparent effector site concentration, a strong increase of power in the beta (especially beta-1) band occurs, accompanied by a moderate increase in delta power. This stage is followed by a decrease in beta power, a further increase of delta power, and a strong increase in alpha power. Finally the power in most bands decreases to very small values, with delta power still increasing towards a final value.

The appearance of the EEG with increasing effector site concentrations first changes from baseline to a dominant beta rhythm with underlying small delta activity. Higher effector site concentrations are associated with a combination of delta and alpha activity. This fast alpha activity becomes smaller leaving almost only (very slow) delta activity with some superimposed fast activity (alpha and theta). A typical appearance of propofol EEG is delta activity with superimposed waxing and waning alpha.

For high effector site concentrations burst suppression occurs with bursts consisting of slow delta waves with some superimposed fast activity from the alpha and theta bands (see next section on burst suppression).

[Veselis-92] gives exact values for the power in each frequency band, for four different electrodes (F_z, C_z, P_z, and O_z). These values show that the change in power is different for each electrode. The value of the power in each band averaged over different channels, as given in most articles, will

therefore not be completely representative for the change in mean power per band at the C_z electrode.

The retained articles give a good impression of the different stages of propofol anesthesia, but mostly do not present quantitative information about the power or amplitude in the different bands. Other articles which give exact numbers for the power or amplitude of the different bands, do not contain information about predicted effector site concentrations or steady state plasma concentrations. Some articles do describe the exact dosing scheme of propofol, which makes it possible to estimate the effector site concentration, using a pharmacokinetic model (see previous section).

From the articles [Kishimoto-95], [Traast-95], [Veselis-92], and[Veselis-93] useful quantitative information was extracted. Except for [Traast-95], in which sufentanil was administered besides propofol, all articles describe the effects of propofol alone. In [Traast-95] sufentanil was administered as a small bolus at the beginning of the procedure, whereas the measurement for the steady state propofol plasma concentration was performed at the end, 60-120 minutes later. It is safe to assume that sufentanil did not have any noticeable influence on the EEG at that time. The age of the subjects in the articles is comparable: 25.4 years in [Kishimoto-95], 34.4 (21-41) in [Veselis-92], 19-47 in [Traast-95], and 19-41 in [Veselis-93].

[Kishimoto-95], [Veselis-92] and [Traast-95] give steady state plasma concentrations together with values for the power of the signals in the different bands. In order to obtain an estimate of the gain of each band, the square root of these powers is used.

Besides the values for the power in each band, [Veselis-93] gives an exact description of the administration of propofol, making it possible to predict the effector site concentration, using the pharmacokinetic model described in the previous section. (A bolus of 0.5 mg/kg propofol was followed by an infusion at 75 μg/kg/min until a total dose of 3.5 mg/kg had been administered. The pharmacokinetic model, described in the previous section, predicts an effector site concentration of 2.0 mg/l at the end of infusion, when the EEG was recorded.) The information extracted from these articles is summarized in table 6.2. For the range from 0 to 1.1 mg/l for the effector site concentration, the information from [Veselis-92] is used, since he gives absolute values for the amplitude in the different bands, instead of a graph of relative values, given by [Kishimoto-95].

Table 6.2: EEG gains for different effector site concentrations. Ce stands for the propofol effector site concentration.

source	Ce (mg/l)	delta (μV)	theta (μV)	alpha (μV)	beta-1 (μV)	beta-2 (μV)
[Veselis-92]	0.86	85.3	31.1	53.2	39.5	25.7
[Veselis-93]	2.02	130.3	42.7	56.2	55.0	40.3
[Traast-95]	3.2	194	52	100	7	7

For effector site concentrations above 3.2 mg/l, the gains have to be estimated. Suttmann shows an illustration of a real EEG just before appearance of burst suppression, which can be used to estimate the gains for higher effector site concentrations.

The effector site concentration at which this EEG is observed is unknown and has to be estimated. In section 6.2 the effector site concentration for onset of burst suppression is predicted to be 4.8

mg/l. Supposing the above described stage of the EEG occurs just before onset of burst suppression, the concentration at which this stage is reached is set at 4.5 mg/l.

A comparison between a real EEG from [Suttmann-89] and a simulated EEG associated with an effector site concentration of 3.2 mg/l was done to estimate the gains at the higher concentrations. From both EEG traces the amplitudes of the different frequency components of the signal are visually estimated and compared. The relative change in band gain is set to be equal to the relative change in average amplitude. The band gains associated with the EEG from Suttmann are calculated by multiplying the gains of the EEG at 3.2 mg/l with this relative change in amplitude. The resulting estimates for the gains are shown in table 6.3.

Table 6.3: Estimates for the gains before and during burst suppression.

source	Ce (mg/l)	delta (μV)	theta (μV)	alpha (μV)	beta-1 (μV)	beta-2 (μV)
[Suttmann-89]	4.5	400	30	20	0	0

The gains during the bursts of burst duration are assumed to be equal to the gains just before burst suppression.

The four points described in tables 6.2 and 6.3 are linearly interpolated to get a continuous effector site concentration-gain curve. (See figure 6.1) Baseline gains are from [DeBeer-97,I].

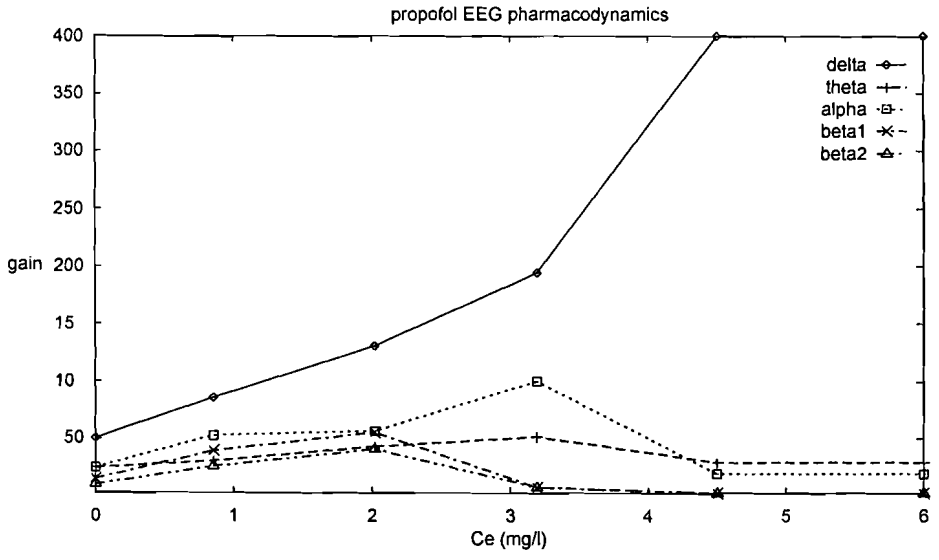

Figure 6.1: Effector site concentration-gain curves for propofol.

modeling burst suppression

As stated in [Jäntti-93], there is no detailed analysis available in the literature of burst suppression patterns during propofol anesthesia. Some information about propofol burst suppression was found in the following articles: [Bendriss-90], [Cheng-96], [Illievich-93], [Newman-95], [Schultz-95],

[Stone-96], [Suttmann-89], [VanHemelrijck-90], and [VanHemelrijck-92], but must of this information is incomplete for the purpose of burst suppression modeling.

[Schultz-95] describes the influence of age on propofol burst suppression. Older subjects show burst suppression at a lower dose of propofol than younger subjects. A higher clearance for younger subjects may be the explanation of this observation. [Cheng-96] shows a large inter-patient variability in the dose of propofol needed to induce burst suppression. The dose varies from 1.5 to 10.2 mg/kg between the different patients. This variability cannot be explained by the age of the patients. [VanHemelrijck-90] and [VanHemelrijck-92] show that nitrous oxide, given in combination with propofol, lowers the threshold for burst suppression.

Considering the above properties of burst suppression after propofol administration, age dependency, other inter-patient variablility, and the effect of nitrous oxide in combination with propofol, only one article contains useful quantitative information about burst suppression characteristics and propofol effector site concentration. [VanHemelrijck-92] gives a steady state propofol plasma concentration of 4.8 mg/l at the onset of burst suppression. Other articles, such as [Cheng-96] contain parts of raw EEGs that show burst suppression. [Illievich-93] and [Bendriss-90] give values for steady state propofol concentrations, but do not contain information about the looked forburst suppression parameters: average suppression duration and average number of bursts per minute.

Concerning the visual appearance of the bursts, the articles mention slow delta waves with some superimposed fast activity from the alpha and theta bands.

In the process of propofol integration, the model for burst suppression was modified. Therefore, no parameters for burst suppression for the existing model were derived (see next section).

6.2 Initial Simulation Results and Model Modifications

pharmacokinetics

After setting the parameters of the pharmacokinetic model according to [Kirkpatrick-88], the propofol plasma concentration after administration of a bolus of 2.5 mg/kg of propofol was simulated. The bolus was equal to the bolus used for the generation of the propofol plasma concentration curve found in [Kirkpatrick-88]. The plasma concentrations of the simulation were similar to those of that curve, indicating that the pharmacokinetic model was implemented correctly and can be used for the EEG simulation development.

gains

The effector site concentration-gain curves determined in section 6.1 were implemented in the EEG simulator. In figure 6.2 a simulation of a single 7 mg/kg bolus of propofol, using these curves is shown. Next to the simulation results some segments of real EEGs from [Suttmann-89] recorded during successive stages of propofol induction are shown, in order to be able to compare the simulated EEG with a real EEG. The effector site concentrations associated with the segments of the real EEG are not known. They are placed according to their similarity with the simulated signal (and not according to their unknown time of occurence).

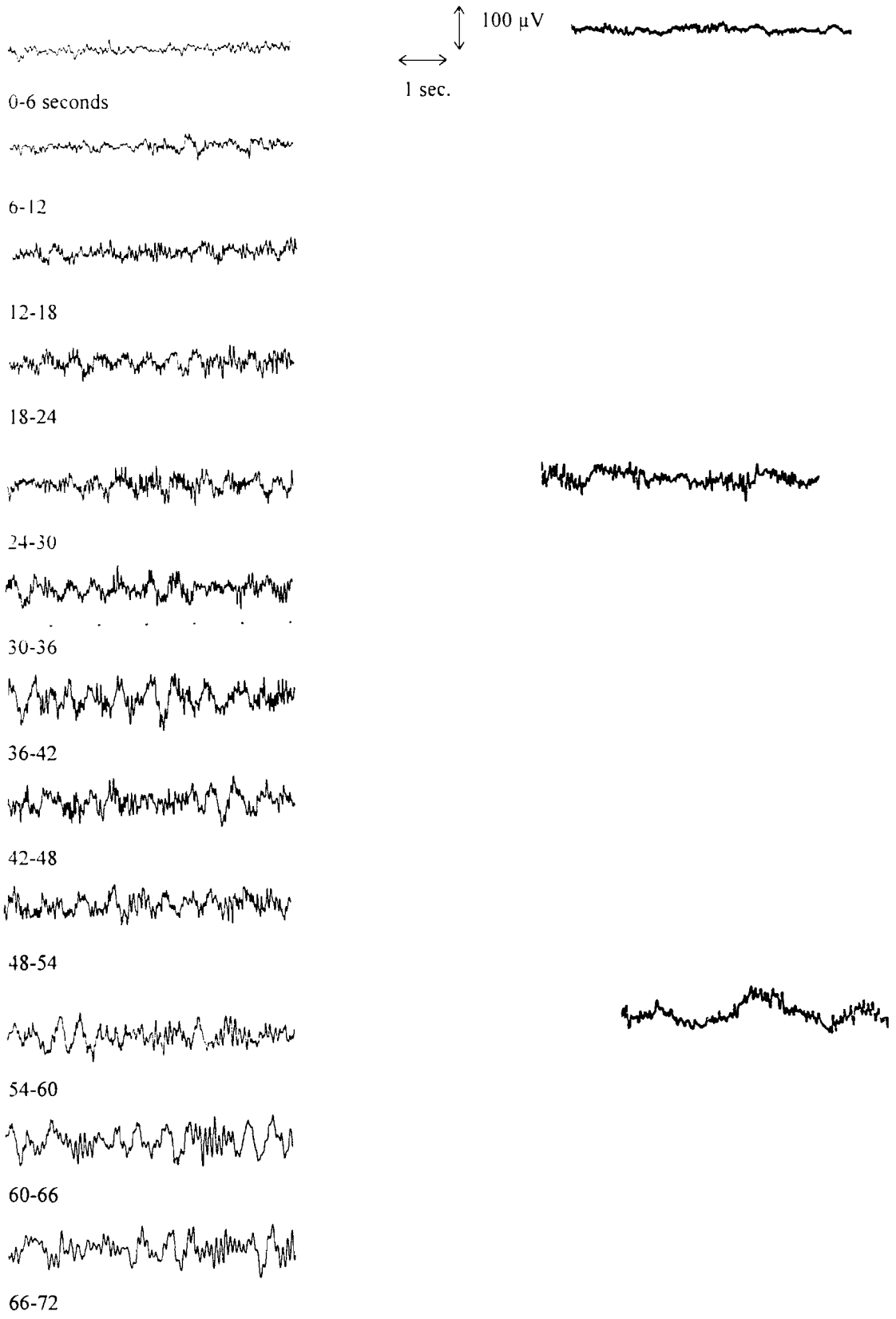

Figure 6.2.a: Simulation of the effects of a 7 mg/kg propofol bolus. See text for explanation of different signals. Permission for actual EEG recordings granted by publisher.

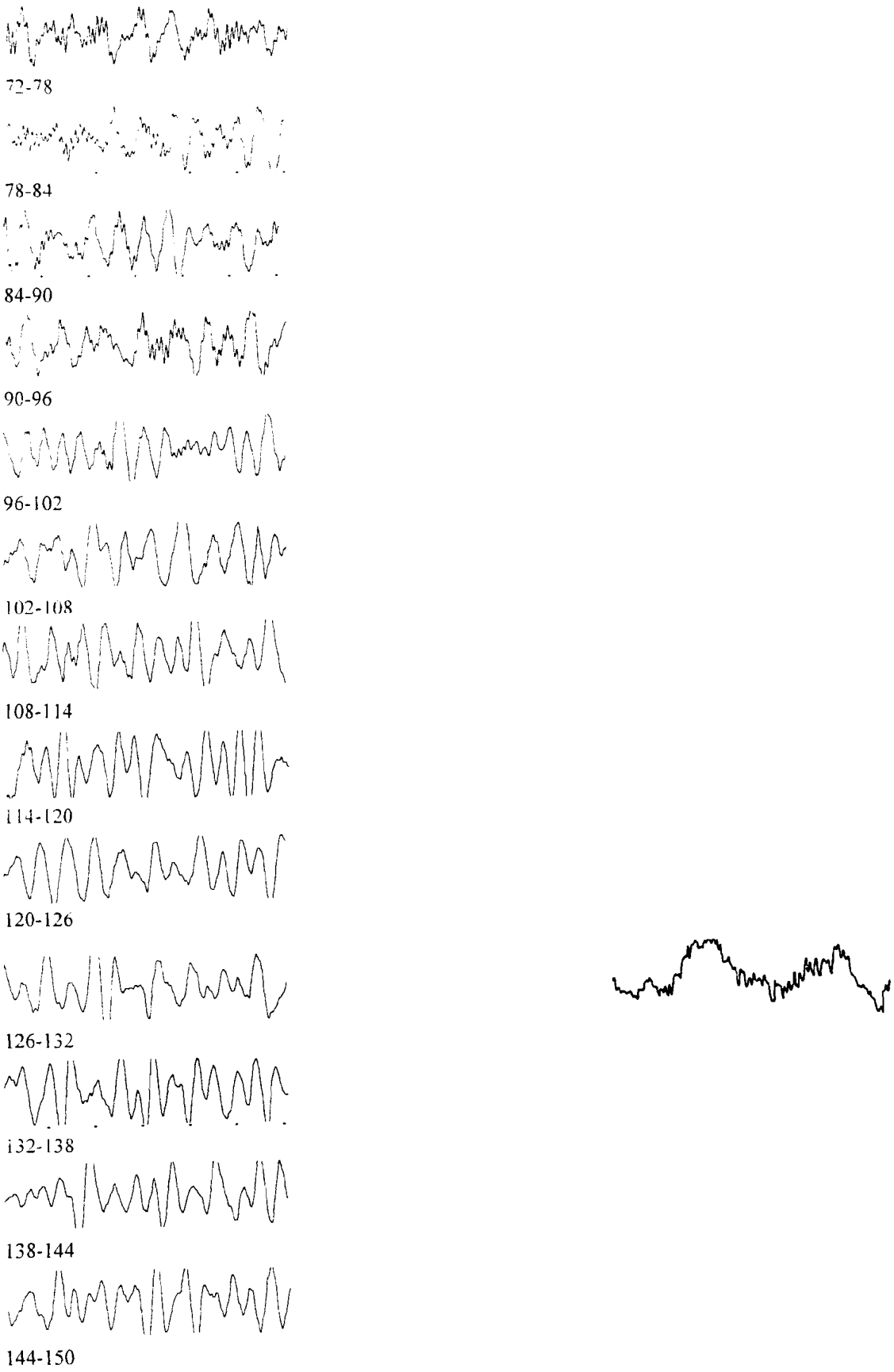

Figure 6.2.b: Simulation of the effects of a 7 mg/kg propofol bolus. See text for explanation of different signals. Permission for actual EEG recordings granted by publisher.

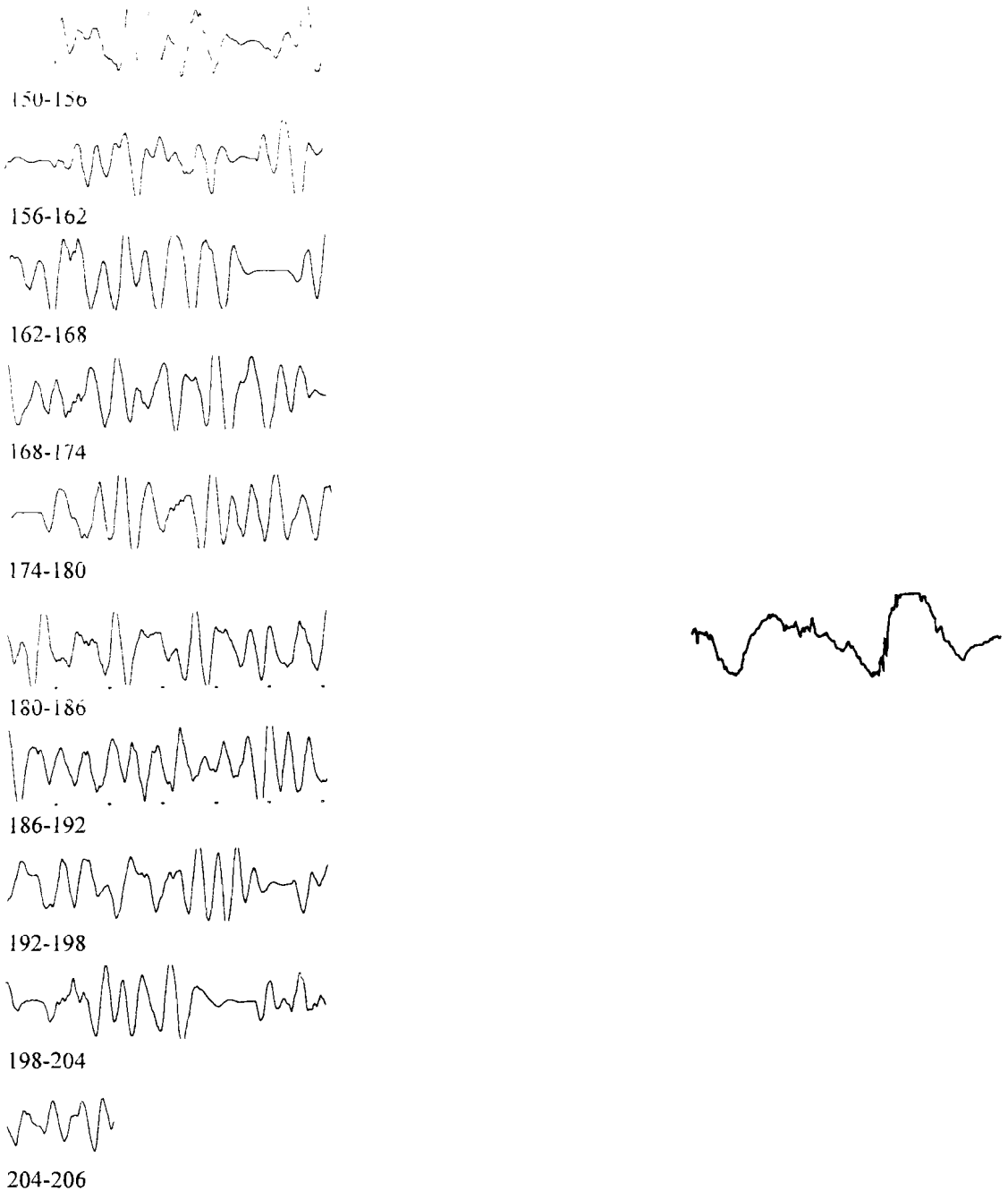

Figure 6.2.c: Simulation of the effects of a 7 mg/kg propofol bolus. See text for explanation of different signals. Permission for actual EEG recordings granted by publisher.

One of the most striking differences between the simulated and the real EEG is the difference in delta activity. In the simulated signal, delta mainly consists of 2 Hz activity, whereas in the real EEG, delta consists of 0.5-1 Hz activity. In addition, the waxing and waning alpha, that seems to be typical for propofol EEGs, can be seen in the simulated signal, but is not very apparent. Otherwise, the stages in the simulated EEG correspond to the descriptions summarized in section 6.1.

modification to the basic model

The difference in delta activity can be reduced by (1) changing the fixed values for the bandwidth and center frequency of the delta band filter (see section 4.1 and 4.2), (2) making the bandwidth and/or center frequency a variable of the type of administered drug, or (3) by making the bandwidth and/or center frequency a variable of the effector site concentration.

The delta activity in the simulated propofol EEG seems to be faster at all stages of induction. Therefore, it will be sufficient to change the fixed parameters for simulation of the effects of propofol (according to option (1)). An expert evaluation has to reveal whether further improvements, in the form of the other two possibilities, is necessary.

For the determination of the new values for the fixed parameters, the original source [Pichlmayr-85] for the parameters for EEG peaks can be used. An EEG peak is chosen with typical slow delta activity. Its bandwidth was determined and new values for a, b, and N were estimated. The resulting filter is a lowpass filter with a bandwidth of 1.04 Hz, which is obtained with values a = 0, b = 0.125, and N=241.

burst suppression

The original model for burst suppression described in section 4.3 requires many parameters that have to be derived from the scientific literature. This makes it difficult or even impossible to obtain a complete set of parameters for burst suppression.

In order to first obtain a good conception of the clinical aspects of burst suppression, Dr. M.E. Mahla [Mahla-97], an anesthesiologist with much EEG monitoring experience, was asked for his input. From these conversations it became clear that burst suppression during anesthesia is only encountered in two cases. First, burst suppression can occur when an overdose is administered. The infusion rate will then be lowered and the burst suppression will rapidly disappear. Second, burst suppression can be induced on purpose, in order to protect the brain during operations where oxygenation of the brain is at risk. In that case anesthesia is controlled to achieve a certain ratio of suppression, usually around 80-90%. If the administered drug dose is too big, total isoelectricity is obtained. The ratio is calculated with the equation:

$$\textit{suppression ratio} = \frac{ASD}{ASD + ABD} \qquad (6.2)$$

According to Dr. Mahla, the average suppression duration (ASD) increases with increasing effector site concentration, whereas the average burst duration (ABD) decreases. He is not familiar with the dependency of the number of suppression periods per minute on the effector site concentration. The model of section 4.3 does not show a correct behavior for the suppression ratio: suppression ratio increases asymptotically with increasing effector site concentration, instead of reaching 100% suppression for a normal overdose. From the conversation with Dr. Mahla, it can be concluded that it is important that all three parameters, suppression duration, burst duration, and suppression ratio, depend realistically on effector site concentration. The onset of burst suppression has to look realistic (in case of overdosing) and the ratio has to evolve from 0 to 1 (or 0 to 100%).

The information from the conversations summarized above is used to modify the existing burst suppression model. The suppression ratio is modeled as linearly increasing with effector site concentration from the concentration associated with the onset of burst suppression to the concentration where isoelectricity first occurs:

$$
\begin{aligned}
ratio(c_e) &= 0 && c_e \le c_{on} \\
ratio(c_e) &= S_r \bullet (c_e - c_{on}) && c_{on} \le c_e \le c_{iso} \\
ratio(c_e) &= 1 && c_e \ge c_{iso}
\end{aligned}
\tag{6.3}
$$

where c_{on} is the effector site concentration of burst suppression onset, and c_{iso} the effector site concentration where total isoelectricity first occurs. If c_{on} and c_{iso} are known, the parameter S_r can be calculated.

$$
S_r = \frac{1}{c_{iso} - c_{on}} \tag{6.4}
$$

Assuming the average burst duration decreases linearly with concentration and is zero at c_{iso} , it can be written as:

$$
ABD(c_e) = -S_b \bullet (c_e - c_{iso}) \qquad c_{on} \le c_e \le c_{iso} \tag{6.5}
$$

in which S_b is a constant.

Combining the equations for the ratio and the burst duration (equations 6.2 through 6.5), the following equation for the average suppression duration results:

$$
ASD(c_e) = S_b(c_e - c_{on}) \qquad c_{on} \le c_e \le c_{iso} \tag{6.6}
$$

The combination of the equations for the ratio, suppression duration, and the burst duration meet all the requirements: The ratio changes from 0 to 1 with increasing effector site concentration, the burst duration decreases, and the suppression duration increases. From the literature, values have to be found or estimated for c_{on}, c_{iso}, and S_b. These parameters can be extracted using the concentration dependency of any of two values of the set {ASD, ABD, ratio, number of bursts per minute}. For the old implementation of the burst suppression model, four parameters had to be estimated.

The parameters for the modified burst suppression model are extracted from the scientific literature. As mentioned before, there is not much information available on burst suppression caused by propofol alone. Especially nitrous oxide seems to have an important effect on the relation between burst suppression and propofol concentrations. From [VanHemelrijck-92] the value c_{on} = 4.8 mg/l can be taken. With ASD(c_e=6.3) = 4 s, the value for the parameter S_b can be calculated: S_b = 2.67 (sl/mg, seconds liter per milligram).

An illustration of a propofol burst suppression pattern is given in [Cheng-96]. From this illustration an ASD of 3.5 s and an ABD of 4 s can be extracted. Combining the equation for the suppression duration with the values for S_b and c_{on} taken from [VanHemelrijck-92], the effector site concentration can be calculated: c_e = 6.1 mg/l.

Combining ABD(c_e=6.1) = 4 s with the value found for S_b, c_{iso} can be calculated: c_{iso} = 7.6 mg/l.

[Illievich-93] mentions steady state plasma concentration of 7-9 mg/l at a burst suppression level of propofol. Most of the cases of burst suppression occur at concentrations higher than the c_{iso} calculated above (7.6 mg/l). Bendriss mentions a steady state plasma concentration of 5.5 mg/l for

suppression durations of 4-6 seconds. Both values do not fit the curve deducted above, although the age groups are very similar. This can be caused by a number of reasons. Burst suppression appears in a rather undeterministic fashion. If the average suppression duration at a certain moment has a certain value, the actual durations vary strongly around that value. This makes it very hard to exactly describe the variables ASD and ABD. Also, the amount of propofol needed to induce burst suppression varies strongly per person [Cheng-96]. Since the goal of the EEG simulator is to simulate a possible person, the current values for the parameters can be used for the burst suppression model. An EEG expert has to judge the reality value of the resulting signal.

6.3 Expert Evaluation of the Updated Model

gains

After implementing the new filter coefficients, with the slower delta, the EEG after administration of a 7 mg/kg bolus of propofol was simulated again. The result is shown in figure 6.3.

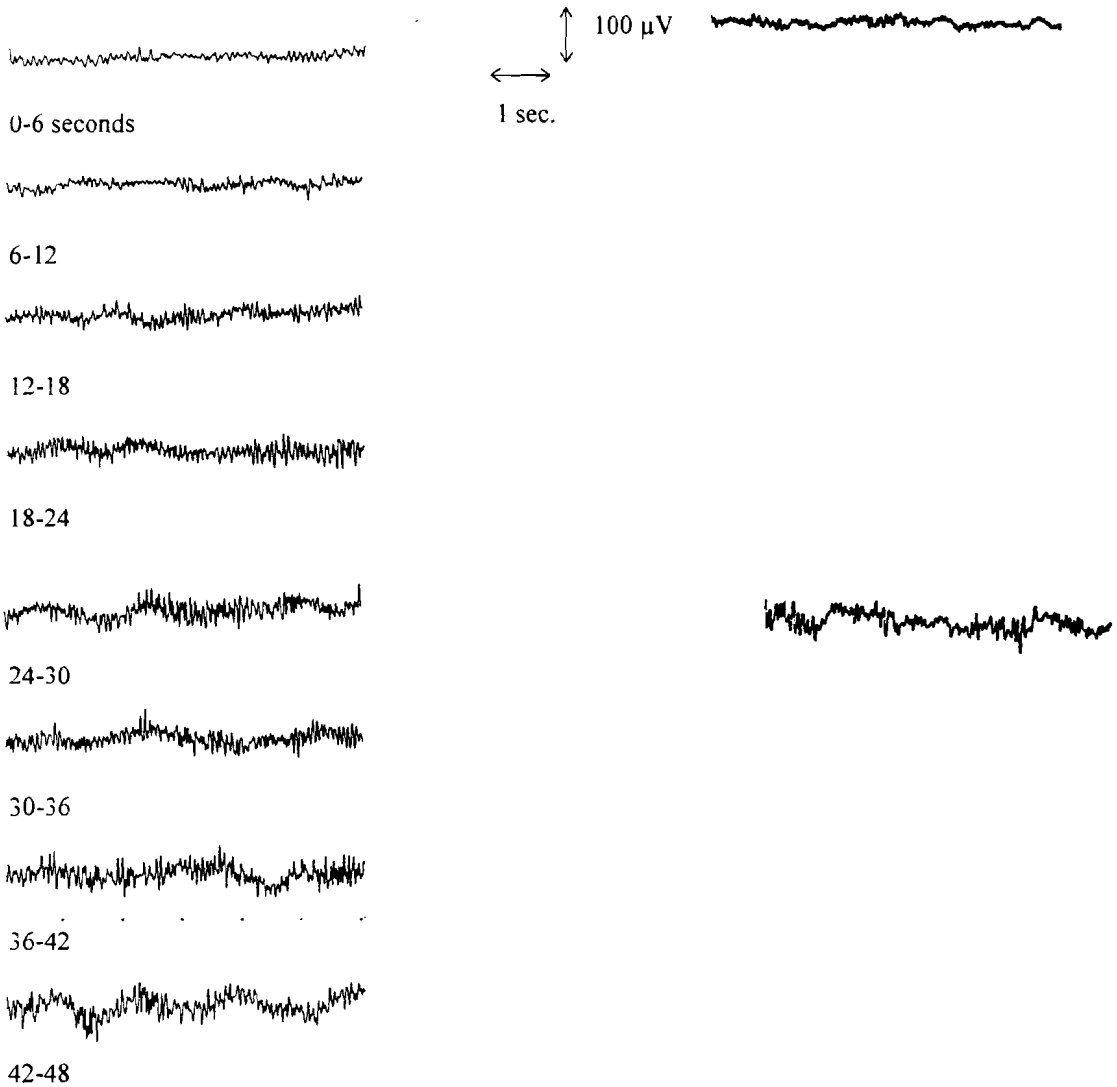

Figure 6.3.a: Simulation of a 7 mg/kg propofol bolus with updated delta filter. See text for explanation of different signals. Permission for actual EEG recordings granted by publisher.

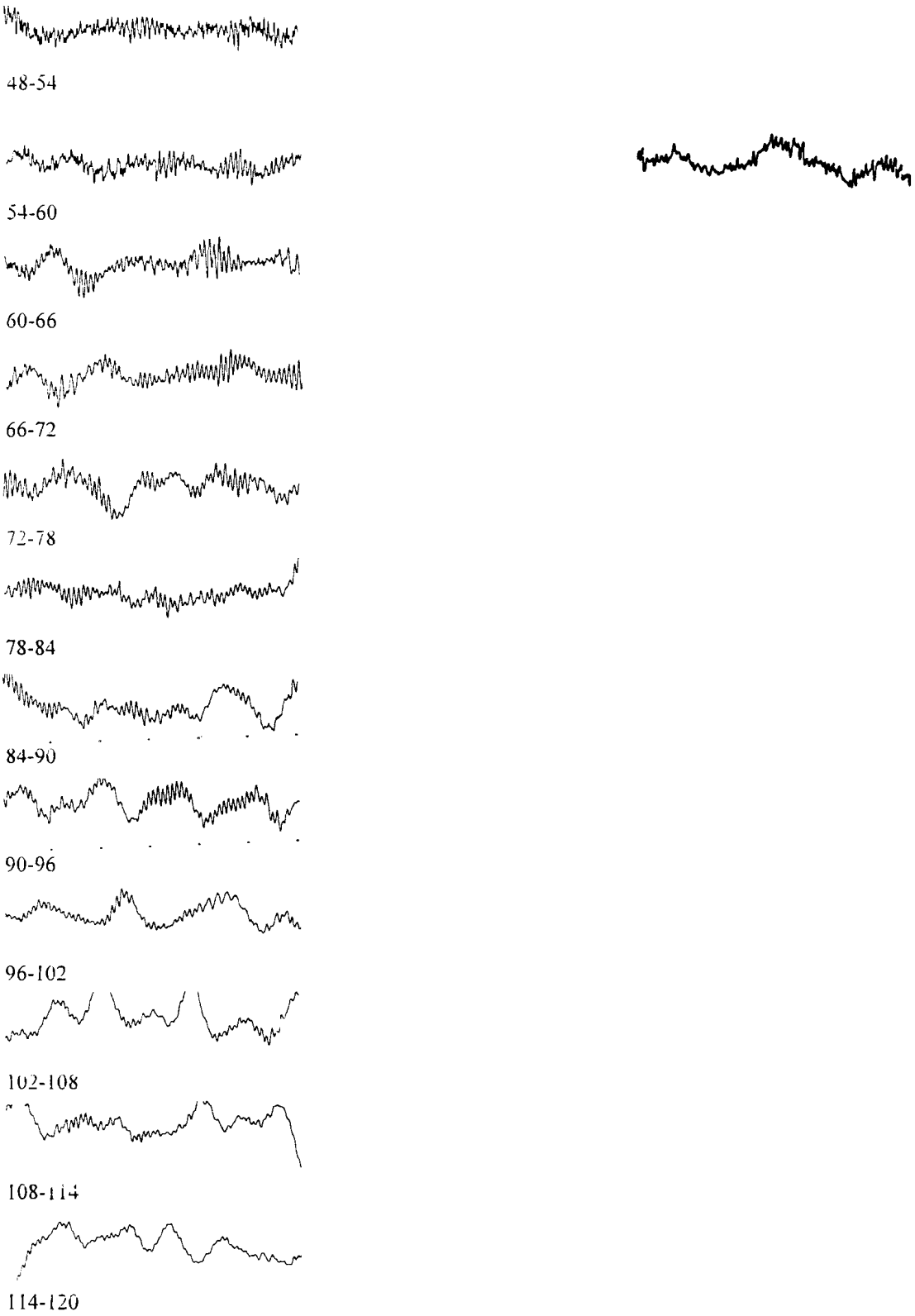

Figure 6.3.b: Simulation of a 7 mg/kg propofol bolus with updated delta filter. See text for explanation of different signals. Permission for actual EEG recordings granted by publisher.

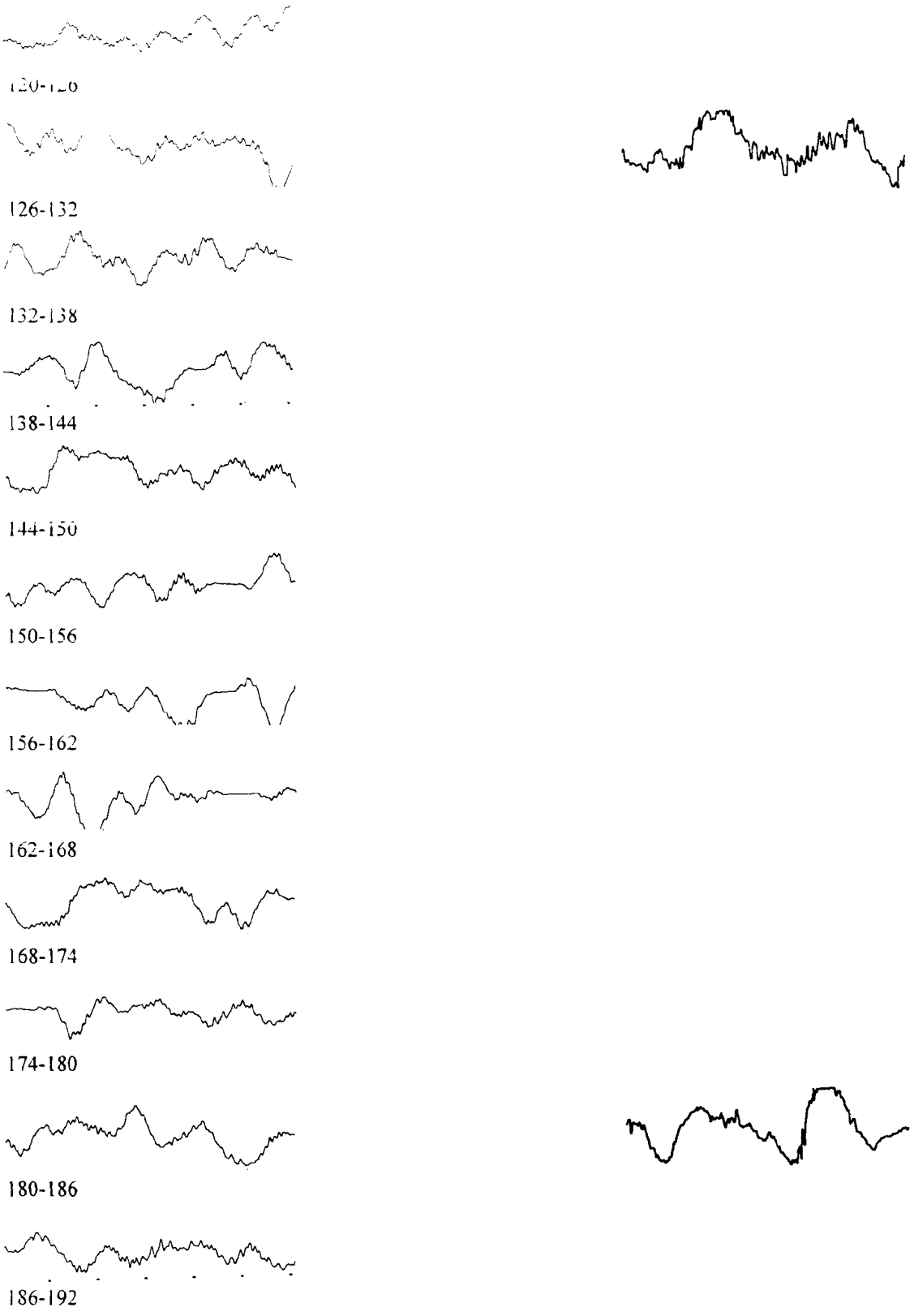

Figure 6.3.c: Simulation of a 7 mg/kg propofol bolus with updated delta filter. See text for explanation of different signals. Permission for actual EEG recordings granted by publisher.

192-198

198-204

204-206

Figure 6.3.d: Simulation of a 7 mg/kg propofol bolus with updated delta filter. See text for explanation of different signals. Permission for actual EEG recordings granted by publisher.

This simulation shows the typical slow delta activity seen in EEGs after propofol administration. This is particularly clear in the last part of the simulation, where delta activity is most dominant. The change of the delta filter characteristics had a positive effect on the appearance of the EEG. Therefore, it should be considered to change the delta filter in the current model for simulation of propofol effects. The waxing and waning alpha activity, that is so typical for propofol is also more clear in this simulation (see for example seconds 60-66 and 90-96).

The simulation with the new delta filter was shown as depicted in figure 6.3 to three anesthesiologists with EEG monitoring experience. The anesthesiologists were asked for their opinion on the realism of the simulated signals, and the usability for educational purposes. This resulted in the following statements:

Some of the stages of the simulated propofol EEG signal look very realistic, for example, the final stage with the high amplitude delta with alpha (and theta) on top. The appearance of the simulated signal in that stage is very similar to the corresponding stage of a real propofol EEG.

For EEG experts with a lot of EEG monitoring experience, the simulator output is not indistinguishable from real. The onset is too fast. In real humans, the distribution via blood to the brain, the crossing of the blood-brain barrier, etc., cause a delay between the administration of the drugs and the effect. After initial onset the trends in the simulation progress too slowly, meaning that the period with beta activity should end earlier and the delta component should appear earlier. The trace at around 130 seconds would typically appear at around 18 seconds, if the onset is as in the print-out. 7 mg/kg is a big bolus. Normally a bolus of 2 mg/kg is used for induction.

The simulator output could be *an* EEG of a possible patient. That patient would probably have a bad heart, resulting in a slow distribution of the drug in the body and a slow progress of the different stages of the EEG. This does not explain the short onset time.

The simulated signal bears enough resemblance to real EEGs for education of residents. Because of the mentioned deviations of the simulation from reality, the signal might not be sufficiently realistic for anesthesia fellows and certainly not for people who have much experience with EEGs.

A possible explanation for the fast onset of the simulated effects of propofol on the EEG lies in the pharmacokinetic model. Drug distribution is modeled with a compartment model. This model results in an effector site concentration that increases immediately after administration of a drug, whereas in reality the drug only reaches the receptors in the brain after some time, since it has to be distributed via the blood to the brain (passing 3/4 of the vascular system), and pass the blood-brain

barrier. Another explanation lies in the piece-wise linear approximation of the pharmacodynamics. The estimated piece-wise linear effector site concentration-gain relationships of figure 6.1 show an immediate increase in all bands for effector site concentrations just above zero. This immediate increase is the result of the linear interpolation of the baseline values and the values at 0.86 mg/l. In addition, the baseline values are taken from other sources than the propofol values. Information about low-dose propofol effects on the EEG in [Kishimoto-95] show that for low effector site concentrations the power in the different bands does not change. It is only for propofol effector site concentrations between 0.2 and 0.3 mg/l, that beta markedly starts to increase. The power in other bands does not change noticeably until the effector site concentration has reached 0.6 mg/l. This threshold for effects on the gains of the different frequency bands could be implemented in the pharmacodynamic model used for the EEG simulator.

From the above determination of explanations, the following solutions to the slow onset can be derived: The piece-wise linear pharmacodynamic relation between the amplitude in the bands and the effector site concentration could be altered for low concentrations. The gains could be made constant for these concentrations, resulting in a slower onset after bolus administration. The pharmacokinetic relation between administration of propofol and the effector site concentration can be influenced by changing k_{e0}. Decreasing k_{e0} will result in a slower increasing effector site concentration. However, altering this parameter will also skew the predicted effector site concentrations. An improvement of the general model for pharmacokinetics, reflecting more realistically the processes in the human body, may be necessary to overcome the problem of the fast onset.

The slow transition from beta activity to delta activity could be caused by the pharmacokinetic model. Although the effect of propofol shows a large inter-patient variability, the difference between the simulation and normal propofol inductions is too big to be explained by this variability only. A deviation in the pharmacokinetic model could cause effector site concentrations that do not rise fast enough after induction, resulting in a slower transition of stages in the EEG. Another explanation of the slow transition could be that the data found for the pharmacodynamic relation are not accurate. The values for the power in the bandwidths are exact, but the concentrations corresponding with these values had to be estimated. If the concentrations were estimated too high, that would have caused a slower transition between stages.

For the height of the dose, the same explanation as for the slow transitions can be given. A smaller bolus of propofol would suffice to reach all the stages of the propofol EEG if the pharmacokinetic and pharmacodynamic models are changed as suggested for the slow transition.

burst suppression

After implementation of the new burst suppression model, the EEG model was extended with propofol. Since the emphasis of the burst suppression model lies on the dynamic behavior, it is not very useful to show print-outs of burst suppression EEGs to EEG experts. Instead, one EEG expert was asked to make use of a screen-only software version of the EEG simulator. He was asked to induce and maintain burst suppression, and to judge the dynamic behavior of the burst suppression. In addition he was asked to judge the appearance of the bursts.

In the expert's opinion, the dynamic behavior of the burst suppression looks very realistic. The variance in burst and suppression duration is realistic (although some bursts are too short) and the average burst suppression ratio changes realistically with changing administration of propofol. The visual appearance of the bursts is realistic. A slight increase in alpha activity might be required. Some of the bursts are too short. In reality short bursts hardly occur. Every now and then some of the delta activity is still too fast. Other bursts show the correct slow delta waves.

Since a large inter-patient variability exists for the onset of burst suppression, it is not possible to judge the concentration at which burst suppression occurs. The evaluation showed that the simulation presents a possible burst suppression pattern. The short duration of some bursts can be avoided by increasing the minimum duration of bursts (see section 5.2).

7. Conclusions and Recommendations

- The learning objectives for a neurophysiological module of a full-scale patient simulator were derived from educational and simulator design considerations. These learning objectives apply to anesthesia training in an OR environment. Future extension of the applications of the module will require reconsidering these learning objectives.
- The design of an existing model-driven EEG simulator model was summarized. This simulator is based on an empirical frequency domain description of the EEG signal., rather than a simulation of the neuronal structure underlying the signal. The EEG signal is obtained by filtering a Gaussian white noise in each of the conventional EEG bands, each with its independent variable gain. This allows independent variation of the power or amplitude in each of the bands. Formal clinical evaluation during the ongoing development of the EEG simulator has to prove whether additional filter parameters, such as the center frequency, and the bandwidth, have to be made variable. It may be difficult to obtain estimates for these extra parameters for all possible situations. In addition, the filter coefficients have to be recalculated each sample if the center frequency and the bandwidth are variable, making the signal generator more computationally intensive. Another possibility to improve the EEG simulation is to increase the number of filter bands. In this case, it will also be difficult to obtain the required parameter estimates (the power in each of these smaller bands) from the scientific literature.
- The filters of the signal generation part of the EEG simulator are formally designed and successfully implemented. Peaks in real human EEG spectra are parametrized by their bandwidth and center frequency, and these parameters are used to design the filter frequency characteristics. A narrow ideal bandpass filter, combined with a Hann window are fitted to the peak parameterizations. The resulting filter can be calculated real-time on a PC 486-66 Hz.
According to three anesthesiologists with EEG monitoring experience, selected patterns, simulated with the EEG signal generator with the described filter characteristics look like typical EEGs and bear enough resemblance to actual EEGs to be used for educational simulation.
The description of real EEG peaks with two parameters, results in an approximation of these real EEG peaks. A description with more parameters would result in a better approximation, but it will be difficult to find estimates for these parameters in the scientific literature, especially when estimates for a variety of conditions are needed. Evaluation of simulations of the effects on the EEG of new independent variables, or of new combinations of variables has to show if improvements in this field are necessary.
No analytically solvable function for the filter coefficients based on the filter characteristics and meeting all other filter requirements could be found. If future evaluations show that it is necessary to make the filter characteristics variable, a look-up table of the relation between the characteristics and the coefficients, or a mathematical approximation of this relation can be implemented. When the filter parameters are known, the filter coefficients can then be calculated from the equations describing the ideal band pass and the Hann window.
- The current insights in pharmacokinetic and pharmacodynamic modeling are summarized from an engineering perspective. The pharmacokinetic part of the EEG simulator is based on these insights. A traditional compartment model is used in the existing EEG simulator to predict the apparent effector site concentration. After completion of the design phase, the EEG simulator will

be integrated into the HPS. The effector site concentration will then be calculated by the HPS in a similar way.

- The important intravenous hypnotic propofol is successfully integrated into the EEG simulator. The simulation results load to a shift in the delta band filter characteristic towards lower frequencies. After this modification of the basic signal generator, the dynamic behavior of the EEG signal after administration of propofol is very realistic. The visual appearance of each of the stages of the EEG is very realistic. According to three anesthesiologists with EEG monitoring experience, the time-course of the changes between the different stages is realistic enough for educational simulation of the effects of drug on the EEG, but needs some improvement in order to become more realistic. Possible improvements include changes of the pharmacokinetic and pharmacodynamic relationships.
- A new model was developed for the simulation of burst suppression. Suppression ratio, suppression duration, and burst duration are modeled as a linear function of the effector site concentration. According to an EEG expert, the appearance of burst suppression can be realistically simulated with this model. Therefore, the burst suppression model can be used for educational simulation.
- Two companion papers ([DeBeer-97,I], and [DeBeer-97,II], both submitted to "Medical & Biological Engineering and Computing") include parts of this master project.

Specific recommendations about modifications or extensions for the follow-up of this project are:

- The gains for the different bands of the EEG signal generator are modeled as piece-wise linear functions of the effector site concentration of various drugs. The effects of multiple drugs are assumed to be additive. The data for this model are extracted from scientific literature. No research is performed yet to justify the assumption of additive drug effects. Inclusion of specific receptors in the pharmacodynamic model may facilitate the simulation of non-linear concentration-effect relationships and of (non-linear) drug interactions.
- For the implementation of scenarios like carotid endarterectomy, the EEG simulator has to be extended with at least a second channel to simulate left-right differences caused by damage or hypoxia in parts of the brain. The effects of damage and different stages of hypoxia in the brain have to be modeled as well. This will probably require a model that includes the effects of blood flow and intracranial pressure. The effects of body temperature on the EEG have to be included as well.
- The ultimate educational value of the EEG simulator can only be determined with the help of clinical instructors in an actual training environment followed by a formal evaluation.
- The addition of more drugs to the model will enlarge its field of application.
- Possible future application areas for an EEG simulator, based on the current design, are the simulation of epileptic seizures, EEG monitoring in the ICU after trauma, and EEGs during sleep.

8. References

[Bashkaran-93] A Bashkaran, CD Ferris, RS Sandige. *A sampling and storage system for arbitrary biomedical waveforms.* Biomed. Sci. Instrum. 29: 393-399, 1993.

[Bendriss-90] P Bendriss, HP Stoiber, AC Bendriss-Brusset, P Dabadie, P Erny. *Propofol effects on EEG and relationship with plasma concentration during neurosurgery.* Anesthesiology 73(3A): A203, 1990.

[Billard-97] V Billard, PL Gambus, N Chamoun, DR Stanski, SL Shafer. *A comparison of spectral edge, delta power, and bispectral index as EEG measures of alfentanil, propofol, and midazolam drug effect.* Clin. Pharmacol. Ther. 61: 45-58, 1997.

[Bührer-94] M Bührer, A Mappes, R Lauber, DR Stanski, PO Maitre. *Dexmedetomidine decreases thiopental dose requirement and alters distribution pharmacokinetics.* Anesthesiology 77(2): 226-236, 1994.

[Cheng-96] MA Cheng, R Tempelhoff, DL Silbergold, MA Theard, SK Haines, JW Miller. *Large-dose propofol alone in adult epileptic patients: electrocorticographic results.* Anesth. Analg. 83(1): 169-174, 1996.

[DeBeer-96] NAM de Beer. *Monitoring adequacy of anesthesia using spontaneous and evoked electroencephalographic activity.* Ph.D. Thesis Eindhoven University of Technology, ISBN 90-386-0317-7, 1996.

[DeBeer-97,I] NAM de Beer, WL van Meurs, MBM Grit, ML Good, D Gravenstein. *Educational simulation of the electroencephalogram (EEG). I: Basic model.* Submitted, 1997.

[DeBeer-97,II] NAM de Beer, WL van Meurs, D Gravenstein, ML Good, MBM Grit. *Educational simulation of the electroencephalogram (EEG). II: Drug effects.* Submitted, 1997.

[Frenkel-95] C Frenkel, J Schüttler, H Ihmen, H Heye, K Rommelheim. *Pharmacokinetics and pharmacodynamics of propofol/alfentanil infusions for sedation in ICU patients.* Intensive Care Med. 21: 981-988, 1995.

[Gaba-95] D Gaba. *Simulator training in anesthesia growing rapidly- CAE model born at Stanford.* APSF newsletter, pp. 34-36, fall 1995.

[Good-89] ML Good, JS Gravenstein. *Anesthesia simulators and training devices*, in Pierce EC Jr. (ed): Risk Management in Anesthesia. International Anesthesiology Clinics, vol 27. Boston, Little, Brown: 161-166, 1989.

[Good-93] ML Good, JS Gravenstein. *Training for safety in an anesthesia simulator.* Seminars in anesthesia-practical considerations in aneasthesia vol XII, no 4: pp. 235-250, december 1993.

[Holford-81] NH Holford, LB Sheiner. *Understanding the dose-effect relationship: Clinical application of pharmacokinetic-pharmacodynamic models.* Clin. Pharmacokinet. 6: 429-453, 1981.

[Hull-79] CJ Hull. *Pharmacokinetics and pharmacodynamics.* Br. J. Anaesth. 51: 579-594, 1979.

[Illievich-93] UM Illievich, W Petricek, W Schramm, M Weindlmayr-Goettel, T Czech, CK Spiss. *Electroencephalographic burst suppression by propofol infusion in humans: hemodynamic consequences.* Anesth. Analg. 77(1): 155-160, 1993.

[Jansen-95] BH Jansen, VG Rit. *Electroencephalogram and visual evoked potential generation in a mathematical model of coupled cortical columns.* Biol. Cybern. 73(4): 357-366, 1995.

[Jäntti-93] V Jäntti, A Yli-Hankala, GA Baer, T Porkkala. *Slow potentials of EEG burst suppression pattern during anaesthesia.* Acta Anaesthesiol. Scand. 37(1): 121-123, 1993.

[Kearse-89] LA Kearse, NR Fahmy. *The electroencephalographic effects of propofol anesthesia in humans: a comparison with thiopental/enflurane anesthesia.* Anesthesiology 3A: A120, 1989.

[Kearse-94] LA Kearse, P Manber, N Chamoun, F deBros, A Zaslavsky. *Bispectral analysis of the electroencephalogram correlates with patient movement to skin incision during propofol/nitrous oxide anesthesia.* Anesthesiology 81: 1365-1370, 1994.

[Kirkpatrick-88] T Kirkpatrick, ID Cockshott, EJ Douglas, WS Nimmo. *Pharmacokinetics of propofol (diprivan) in elderly patients.* Br. J. Anaesth. 60: 146-150, 1988.

[Kishimoto-95] T Kishimoto, C Kadoya, R Sneyd, SK Samra, EF Domino. *Topographic electroencephalogram of propofol-induced conscious sedation.* Clin. Pharmacol. Ther. 58(6): 666-674, 1995.

[Lagerlund-88] TD Lagerlund, FW Sharbrough. *Computer simulation of neuronal circuit models of rhythmic behavior in the electroencephalogram.* Comput. Biol. Med. 18(4): 267-304, 1988.

[Lees-96] DE Lees. *Simulators may create hazards in reality.* APSF newsletter (letter to the editor), p. 9, spring 1996.

[Mahla-92] ME Mahla, A Pashayan, BL Grundy, S Mixson, RK Richards, AL Day. *Prolonged anesthesia with propofol or isoflurane: intraoperative electroencephalographic patterns and postoperative recovery.* Semin. Anesth. 11: 31-32, 1992.

[Mahla-97] Michael E. Mahla, MD. Associate Professor of Anesthesiology and Neurosurgery, Assistant Chair for Education. University of Florida College of Medicine. Personal Communications, 1997.

[Mersereau-94] RM Mersereau, MJT Smith. *Digital Filtering, a computer laboratory textbook.* Wiley, 1994.

[Newman-95] MF Newman, JM Murkin, G Roach, ND Croughwell, WD White, FM Clements, JG Reves. *Cerebral physiologic effects of burst suppression doses of propofol during nonpulsatile cardiopulmonary bypass.* Anesth. Analg. 81(3): 452-457, 1995.

[Nikkelen-95] ALJM Nikkelen. *Pharmacokinetic and pharmacodynamic modeling of neuromuscular blocking agents for educational simulation.* M.S.E.E. Thesis, Eindhoven University of Technology, August 1995.

[Oppenheim-89] AV Oppenheim, RW Schafer. *Discrete Signal Processing.* Englewood Cliffs, Prentice Hall, 1989.

[Pichlmayr-85] I Pichlmayr. *EEG Atlas for Anesthesiologists.* Hannover, Springer-Verlag, 1985.

[Reddy-92] RV Reddy, SS Moorthy, T Mattice, SF Dierdorf, RD Deitch. *An electroencephalographic comparison of effects of propofol and methohexital.* Electroencephalogr. Clin. Neurophysiol. 83(2): 162-168, 1992.

[Russell-95] GB Russell, LD Rodichok. *Primer of Intraoperative Neurophysiologic Monitoring.* Newton, Butterworth-Heinemann, 1995.

[Schultz-95] B Schultz, A Schultz, U Grouven, I Zander, I Pichlmayr. *Veränderung des Narkose-EEG mit dem Lebensalter.* Anaesthesist 44: 467-472, 1995.

[Schüttler-85] J Schüttler, H Schwilden, H Stoeckel. *Pharmacokinetic-dynamic modeling of diprivan.* Anesthesiology 65(3A): A549, 1986.

[Schwilden-89] H Schwilden, H Stoeckel, J Schüttler. *Closed-loop feedback control of propofol anaesthesia by quantitative EEG analysis in humans.* Br. J. Anaesth. 62(3): 290-296, 1989.

[Seiffert-93] HA Seiffert, RT Blouin, PF Conard, JB Gross. *Sedative doses of propofol increase beta activity of the processed electroencephalogram.* Anesth. Analg. 76: 976-978, 1993.

[Sheiner-79] LB Sheiner, DR Stanski, S Vozeh, RD Miller, J Ham. *Simultaneous modeling of pharmacokinetics and pharmacodynamics: Application to d-tubocurarine.* Clin. Pharmacol. Ther. 25: 358-371, 1979.

[Sigl-94] JC Sigl, NG Chamoun. *An introduction to bispectral analysis for the electroencephalogram.* J. Clin. Monit. 10: 392-404, 1994.

[Sneyd-94] JR Sneyd, SK Samra, B Davidson, T Kishimoto, C Kadoya, EF Domino. *Electrophysiologic effects of propofol sedation.* Anesth. Analg. 79(6): 1151-1158, 1994.

[Stone-96] JG Stone, WL Young, ZS Marans, RA Solomon, CR Smith, SC Jamdar, N Opstapkovich, J Diaz. *Consequences of electroencephalographic-suppressive doses of propofol in conjunction with deep hypothermic circulatory arrest.* Anesthesiology 85: 497-501, 1996.

[Suttmann-89] H Suttmann, G Juhl, B Baur, W Morgenstern, A Doenicke. *Visuelle EEG-Analyse zur Steuerung intravenöser Narkosen mit Propofol.* Anaesthesist 38: 180-188, 1989.

[Traast-95] HS Traast, CJ Kalkman. *Electroencephalographic characteristics of emergence from propofol/sufentanil total intravenous anesthesia.* Anesth. Analg. 81(2): 366-371, 1995.

[VandenBosch-94] PPJ van den Bosch, AC van der Klauw. *Modeling, Identification and Simulation of Dynamical Systems.* Eindhoven and Delft, CRC Press Inc., 1994.

[VanderAa-90] JJLCM van der Aa. *Intelligent alarms in anesthesia-a real time expert system application.* Ph.D. Thesis Eindhoven University of Technology. ISBN 90-9003303-3. 1990.

[VanHemelrijck-90] J van Hemelrijck, R Tempelhoff, WS Jellish, PF White. *Use of EEG for determining propofol requirement during neuroanesthesia.* Anesthesiology 3A: A201, 1990.

[VanHemelrijck-92] J van Hemelrijck, R Tempelhoff, P White, W Jellish. *EEG-assisted titration of propofol infusion during neuroanesthesia: effect of nitrous oxide.* J. Neurosurg. Anesth. 4: 11-20, 1992.

[van Meurs-97,I] WL van Meurs, ML Good, S Lampotang. *Functional anatomy of full-scale patient simulators.* In press. 1997.

[van Meurs-97,II] WL van Meurs, E Nikkelen, ML Good. *Pharmacokinetic-Pharmacodynamic model for educational simulations.* Submitted. 1997.

[van Meurs-97,PC] WL van Meurs, Ph.D. Assistant Professor of Anesthesiology. University of Florida College of Medicine. Personal Communications, 1997.

[Veselis-92] RA Veselis, RA Reinsel, M Wronski, P Marino, WP Tong, RF Bedford. *EEG and memory effects of low-dose infusions of propofol.* Br. J. Anaesth. 69(3): 246-254, 1992.

[Veselis-93] RA Veselis, R Reinsel, M Wronski. *Analytical methods to differentiate similar electroencephalographic spectra: neural network and discriminant analysis.* J. Clin. Monit. 9(4): 257-267, 1993.

[Webster's-90] Webster's ninth new collegiate dictionary. Merriam-Webster Inc. publishers. Springfield, Massachusetts, USA. 1990.

[Wilson-92] M Wilson, JM Bower. *Cortical oscillations and temporal interactions in a computer simulation of piriform cortex.* J. Neurophysiol. 67(4): 981-995, 1992.